The Plant Cell, Vol. 13, 1567–1585, July 2001, www.plantcell.org © 2001 American Society of Plant Biologists

# The Last Step of Syringyl Monolignol Biosynthesis in Angiosperms Is Regulated by a Novel Gene Encoding Sinapyl Alcohol Dehydrogenase

**Laigeng Li,[a] Xiao Fei Cheng,[a] Jacqueline Leshkevich,[a] Toshiaki Umezawa,[a,b] Scott A. Harding,[a] and Vincent L. Chiang[a,1]**

[a] Plant Biotechnology Research Center, School of Forestry, Michigan Technological University, Houghton, Michigan 49931
[b] Laboratory of Biochemical Control, Wood Research Institute, Kyoto University, Uji, Kyoto 611-0011, Japan

**Cinnamyl alcohol dehydrogenase (CAD; EC 1.1.1.195) has been thought to mediate the reduction of both coniferaldehyde and sinapaldehyde into guaiacyl and syringyl monolignols in angiosperms. Here, we report the isolation of a novel aspen gene (*PtSAD*) encoding sinapyl alcohol dehydrogenase (SAD), which is phylogenetically distinct from aspen CAD (PtCAD). Liquid chromatography–mass spectrometry-based enzyme functional analysis and substrate level–controlled enzyme kinetics consistently demonstrated that PtSAD is sinapaldehyde specific and that PtCAD is coniferaldehyde specific. The enzymatic efficiency of PtSAD for sinapaldehyde was ~60 times greater than that of PtCAD. These data suggest that in addition to CAD, discrete SAD function is essential to the biosynthesis of syringyl monolignol in angiosperms. In aspen stem primary tissues, PtCAD was immunolocalized exclusively to xylem elements in which only guaiacyl lignin was deposited, whereas PtSAD was abundant in syringyl lignin–enriched phloem fiber cells. In the developing secondary stem xylem, PtCAD was most conspicuous in guaiacyl lignin–enriched vessels, but PtSAD was nearly absent from these elements and was conspicuous in fiber cells. In the context of additional protein immunolocalization and lignin histochemistry, these results suggest that the distinct CAD and SAD functions are linked spatiotemporally to the differential biosynthesis of guaiacyl and syringyl lignins in different cell types. *SAD* is required for the biosynthesis of syringyl lignin in angiosperms.**

## INTRODUCTION

The evolution of modern angiosperms from their gymnosperm progenitors has been marked by important changes in vascular development, including lignification. Lignin in gymnosperms is polymerized primarily from the guaiacyl monolignol, coniferyl alcohol. In angiosperms, the syringyl monolignol, sinapyl alcohol, emerges from the guaiacyl pathway and polymerizes with guaiacyl monolignols to form a heterologous guaiacyl-syringyl lignin (Towers and Gibbs, 1953; Wardrop, 1971). The reductive formation of coniferyl and sinapyl alcohols from coniferaldehyde and sinapaldehyde, therefore, has been considered to be the last step in monolignol biosynthesis, and the reactions are catalyzed by cinnamyl alcohol:$NADP^+$ dehydrogenase (CAD; EC 1.1.1.195) (Mansell et al., 1974, 1976; Kutsuki et al., 1982; Higuchi, 1997).

CAD in gymnosperms is encoded by a single gene, and only one CAD protein isoform has been detected in and purified from lignifying tissues of various gymnosperms (Lüderitz and Grisebach, 1981; O'Malley et al., 1992; Galliano et al., 1993a, 1993b; MacKay et al., 1995; Zinser et al., 1998). Gymnosperm CAD is coniferaldehyde specific with insignificant catalytic activity toward sinapaldehyde (Lüderitz and Grisebach, 1981; Kutsuki et al., 1982; O'Malley et al., 1992; Galliano et al., 1993b), consistent with the biosynthesis of mainly guaiacyl lignin in these species. In contrast, multiple CAD isoforms have been purified from a number of angiosperms (Mansell et al., 1974; Wyrambik and Grisebach, 1975, 1979; Sarni et al., 1984; Goffner et al., 1992; Halpin et al., 1992; Hibino et al., 1993a; Grima-Pettenati et al., 1994; Hawkins and Boudet, 1994). Those considered to be monolignol related exhibited comparable catalytic activities with coniferaldehyde and sinapaldehyde (Kutsuki et al., 1982; Goffner et al., 1992; Grima-Pettenati et al., 1994; Hawkins and Boudet, 1994). This has lent support to a model in which the last step in the biosynthesis of guaiacyl and syringyl monolignols in angiosperms is mediated by a broad specificity CAD capable of reducing both coniferaldehyde and sinapaldehyde (Boudet et al., 1995; Whetten and Sederoff, 1995; Whetten et al., 1998).

[1] To whom correspondence should be addressed. E-mail vchiang@mtu.edu; fax 906-487-2915.

Putative *CAD* cDNA sequences also have been isolated from various angiosperms (Knight et al., 1992; Grima-Pettenati et al., 1993; Hibino et al., 1993b; Van Doorsselaere et al., 1995; Sato et al., 1997; Goffner et al., 1998; Brill et al., 1999). The biochemical functions of the proteins they encode, however, remain largely unknown. Two lucerne cDNAs, *MsaCad1* and *MsaCad2*, were characterized for their protein functions (Brill et al., 1999). *MsaCad1* encoded a benzaldehyde dehydrogenase thought to be associated with pathogen defense (Somssich et al., 1989, 1996). *MsaCad2* was believed to encode a monolignol-related CAD because it catalyzed the reduction of coniferaldehyde and sinapaldehyde but not of benzaldehyde derivatives. It was reported as well that the protein encoded by a putative *CAD* cDNA, *pEuCAD2*, from *Eucalyptus gunnii* used coniferaldehyde and sinapaldehyde equally (Grima-Pettenati et al., 1993). pEuCAD2 shares high amino acid sequence homology (80% identity) with MsaCad2. In fact, all monolignol-related CADs cloned thus far from angiosperms share high protein sequence homology with either MsaCad2 (73 to 80% identity) or pEuCAD2 (79 to 81% identity).

The identification of these homologs appears to support the model of multisubstrate CADs in angiosperms for the biosynthesis of monolignols. The suppression of *CAD* gene expression resulting in an essentially unchanged syringyl-to-guaiacyl (S/G) lignin ratio in transgenic poplar (Baucher et al., 1996) also seems to agree with such a model. However, other transgenic results on CAD downregulation all showed altered S/G ratios (Halpin et al., 1994; Higuchi et al., 1994; Baucher et al., 1996; Stewart et al., 1997), suggesting a likely preferential suppression of substrate-specific alcohol dehydrogenases involved in monolignol biosynthesis. Stewart et al. (1997) showed that CAD-suppressed transgenic tobacco plants had xylem lignin with an increased amount of coniferaldehyde. These results are consistent with the demonstration by Higuchi et al. (1994) that lignins in CAD downregulated transgenic tobacco exhibited up to a 10-fold increase in the quantity of coniferaldehyde, with no change in sinapaldehdye content. Moreover, these transgenic plants had a 24% increase in S/G ratio. These findings are evidence that the downregulated CAD was coniferaldehyde or guaiacyl specific.

In addition, whereas the *Eucalyptus gunnii CAD* gene, *pEuCAD2*, was shown to be highly expressed in developing xylem, it was not expressed in phloem (Grima-Pettenati et al., 1993), a tissue that accumulates syringyl-enriched lignin (Grand et al., 1982). Furthermore, polyclonal antibodies against pEuCAD2 reacted with hybrid poplar proteins localized in stem protoxylem (Samaj et al., 1998), likely a guaiacyl lignin–enriched tissue (Bland, 1966; Hu et al., 1998; Tsai et al., 1998). These results cast doubt on the association of *pEuCAD2*, and therefore its homologs, with the biosynthesis of syringyl monolignol. Together, these lines of evidence led us to hypothesize a new model in which the biosynthesis of monolignols in angiosperms may require guaiacyl-specific as well as syringyl-specific CADs.

The proposition of a syringyl-specific CAD, or sinapyl alcohol dehydrogenase (SAD), also is consistent with recent insights into the mechanism of monolignol substrate biosynthesis. Evidence is accumulating that while being metabolized into guaiacyl monolignol, coniferaldehyde formed in the guaiacyl pathway in angiosperms also becomes a key entry point to sinapaldehyde biosynthesis (Humphreys et al., 1999; Osakabe et al., 1999; Li et al., 2000). Two metabolic steps that are absent from gymnosperm monolignol biosynthesis are linked to syringyl flux. Coniferaldehyde 5-hydroxylase (CAld5H) catalyzes the 5-hydroxylation of coniferaldehyde into 5-hydroxyconiferaldehyde (Osakabe et al., 1999), which in turn is methylated by 5-hydroxyconiferaldehyde *O*-methyltransferase (AldOMT) to form sinapaldehyde (Li et al., 2000). Therefore, the reduction of sinapaldehdye by SAD would be consistent with syringyl monolignol biosynthesis having coevolved with angiosperm-specific CAld5H/AldOMT/SAD functions.

The vascular system in gymnosperms is relatively simple, consisting mainly of tracheid cells for both conduction and strengthening (Esau, 1965). Angiosperm xylem cells evolved from tracheids and differentiated into conducting elements, the vessels, and principal strengthening elements, the fibers (Esau, 1965). Vessels are enriched in guaiacyl lignin, whereas syringyl-enriched lignin is deposited in fibers (Fergus and Goring, 1970a, 1970b; Musha and Goring, 1975; Saka and Goring, 1985). Furthermore, the deposition of guaiacyl lignin precedes that of syringyl lignin in differentiating xylem elements (Terashima et al., 1986; Saka and Goring, 1988). Our hypothesis of the presence of distinct CAD and SAD functions, therefore, could be extended to suggest that CAD and CAld5H/AldOMT/SAD functions may be an evolutionary adaptation of angiosperms linked to the differential biosynthesis of guaiacyl and syringyl lignins in accordance with vascular specialization. CAld5H and AldOMT functions during syringyl monolignol biosynthesis have been confirmed in a variety of angiosperms (Li et al., 2000). However, SAD function has yet to be demonstrated.

We report here the discovery of a *SAD* cDNA, *PtSAD*, in developing xylem of aspen. The PtSAD protein sequence is phylogenetically distinguishable from the sequences of all currently known monolignol CADs. We also cloned an aspen xylem *CAD* cDNA, *PtCAD*. Mass spectrometry–based protein functional analyses with 14 aromatic aldehydes and enzyme kinetics confirmed that PtSAD is sinapaldehyde specific and that PtCAD is coniferaldehyde specific. Protein immunolocalization and lignin histochemical localization further revealed that the distributions of PtCAD and PtCAld5H/PtSAD proteins were correlated spatiotemporally with the deposition of guaiacyl and syringyl lignins in different cell types. Distinct SAD and CAD proteins also were found in several angiosperm species. Together, these results suggest discrete roles in angiosperms for CAD and CAld5H/AldOMT/SAD proteins in coordinating cell-specific biosynthesis of guaiacyl and syringyl lignins.

## RESULTS

### Cloning of a Novel Alcohol Dehydrogenase Gene, *PtSAD*, from Aspen

To test our hypothesis of distinct *CAD* and *SAD* genes in angiosperms, we first cloned a *CAD* cDNA, *PtCAD*, from developing xylem of aspen and used it to screen for related sequences in the same species. Low- and high-stringency differential screening of $2.4 \times 10^4$ plaque-forming units from an aspen xylem cDNA library (Wu et al., 2000) resulted in the isolation of two groups of positive clones. Group I contained 12 cDNAs with sequences identical to *PtCAD*. Sequences of the eight cDNAs constituting group II were identical to each other but differed from *PtCAD*. Two of the eight clones in group II were full-length cDNAs and were tentatively named *PtSAD*.

The open reading frame of PtSAD was 1086 bp, encoding a 39-kD protein with a pI of 6.69. The deduced amino acid sequence of PtSAD was 53% identical to that of PtCAD and ~50% identical to that of other angiosperm monolignol CADs, but it exhibited insignificant identity (10 to 40%) with the sequences of alcohol dehydrogenases (ADHs) associated with pathogen defense (Brill et al., 1999). PtCAD, on the other hand, showed extensive amino acid sequence identity with CADs from *Populus trichocarpa* × *Populus deltoides* (97%) (PtCADA; Van Doorsselaere et al., 1995), *Eucalyptus gunnii* (81%) (pEuCAD2; Grima-Pettenati et al., 1993), tobacco (82%) (pTCAD14; Knight et al., 1992), lucerne (79%) (MsaCad2; Brill et al., 1999), and other reported angiosperms (~80%) (Brill et al., 1999). Therefore, *PtSAD* belongs to a novel class of ADHs.

Cofactor and zinc binding sequences conserved in ADHs (Jornvall et al., 1987) were present in PtSAD (Figure 1). The Zn1 binding motif and structural Zn2 consensus regions (Jornvall et al., 1987; MacKay et al., 1995) were located at amino acid residues 71 to 85 and 91 to 117, respectively. A NADP binding site (Jornvall et al., 1987) was identified at residues 191 to 196. Repeated screening of the aspen xylem cDNA library with either *PtCAD* or *PtSAD* cDNA probes always resulted in the isolation of clones identical to either *PtCAD* or *PtSAD*, indicating that they are the two predominant monolignol-related *ADH*s in lignifying xylem.

Phylogenetic analysis of PtSAD and available full-length monolignol CAD protein sequences showed that gymnosperm and angiosperm CADs form a cluster that does not include PtSAD (Figure 2). The angiosperm monolignol CADs in this cluster share ~70% amino acid sequence identity with gymnosperm CADs but ~50% with PtSAD, suggesting that all of these putative angiosperm monolignol CADs may be guaiacyl specific. These results also may reflect a divergence of the guaiacyl CAD phylogenetic group into a more syringyl-specialized group, to which PtSAD belongs.

### DNA Gel Blot Analysis of *PtCAD* and *PtSAD* and RNA and Protein Gel Blot Analyses of *PtCAD* and *PtSAD* Tissue-Specific Expression in Aspen

To determine whether there are other *PtCAD*- and *PtSAD*-related sequences in aspen, we performed gel blot analysis of aspen genomic DNA digested by various restriction enzymes and hybridized with either *PtCAD* (Figure 3A) or *PtSAD* (Figure 3B) full-length cDNA probes. There was a strong single band in each lane, but a weak single band also was detected in each lane, perhaps evidence of a distantly related sequence. Together with our cDNA screening results, we interpret these data to indicate that *PtCAD* and *PtSAD* likely are the predominant members of a small gene family in aspen.

DNA gel blot analysis also clearly demonstrated that *PtCAD* and *PtSAD* did not cross-hybridize with each other. Thus, using the same hybridization conditions and *PtCAD* and *PtSAD* full-length cDNA probes, we conducted RNA gel blot analysis to investigate the tissue-specific expression of *PtCAD* and *PtSAD* in aspen. The greatest *PtCAD* expression was found in tissue types containing a large amount of lignifying xylem, but its expression was lower in phloem-enriched tissues (internodes 1 to 3; Figure 3C). Strong expression of *PtSAD* was detected in tissues undergoing rapid phloem (internodes 1 to 3; Figure 3D) and xylem (internodes 4 to 9; Figure 3D) development. The expression of *PtCAD* and *PtSAD* was not observed in leaves in which vascular mid-veins were removed.

Next, we conducted protein gel blot analysis to verify the tissue-specific expression of *PtCAD* and *PtSAD*. We obtained polyclonal antisera against affinity-purified PtCAD and PtSAD recombinant proteins produced in *Escherichia coli* and used protein gel blotting to verify the specificity of PtCAD and PtSAD antibodies against PtCAD and PtSAD recombinant proteins. For the various recombinant protein amounts (up to 75 ng) tested, PtCAD antibody did not cross-react with PtSAD protein (Figure 3E), and PtSAD antibody did not cross-react with PtCAD protein (Figure 3F). The PtCAD protein exhibited the expected molecular mass of ~39 kD and was more abundant in protein extracts from xylem than from phloem tissue (Figure 3E). In contrast, the strongest signal using PtSAD antibody was detected in phloem protein extracts (Figure 3F). RNA and protein gel blot analyses consistently indicated that both *PtCAD* and *PtSAD* were associated with lignification. Strong *PtSAD* expression in syringyl lignin–enriched phloem (Grand et al., 1982) suggests a specialized role for *PtSAD* in syringyl monolignol biosynthesis. Therefore, we characterized the biochemical functions of the *PtCAD* and *PtSAD* genes.

### Substrate Specificity of PtCAD and PtSAD with Phenolic Aldehydes

NADPH-dependent CAD reductive activity has been estimated spectrophotometrically by monitoring the decrease

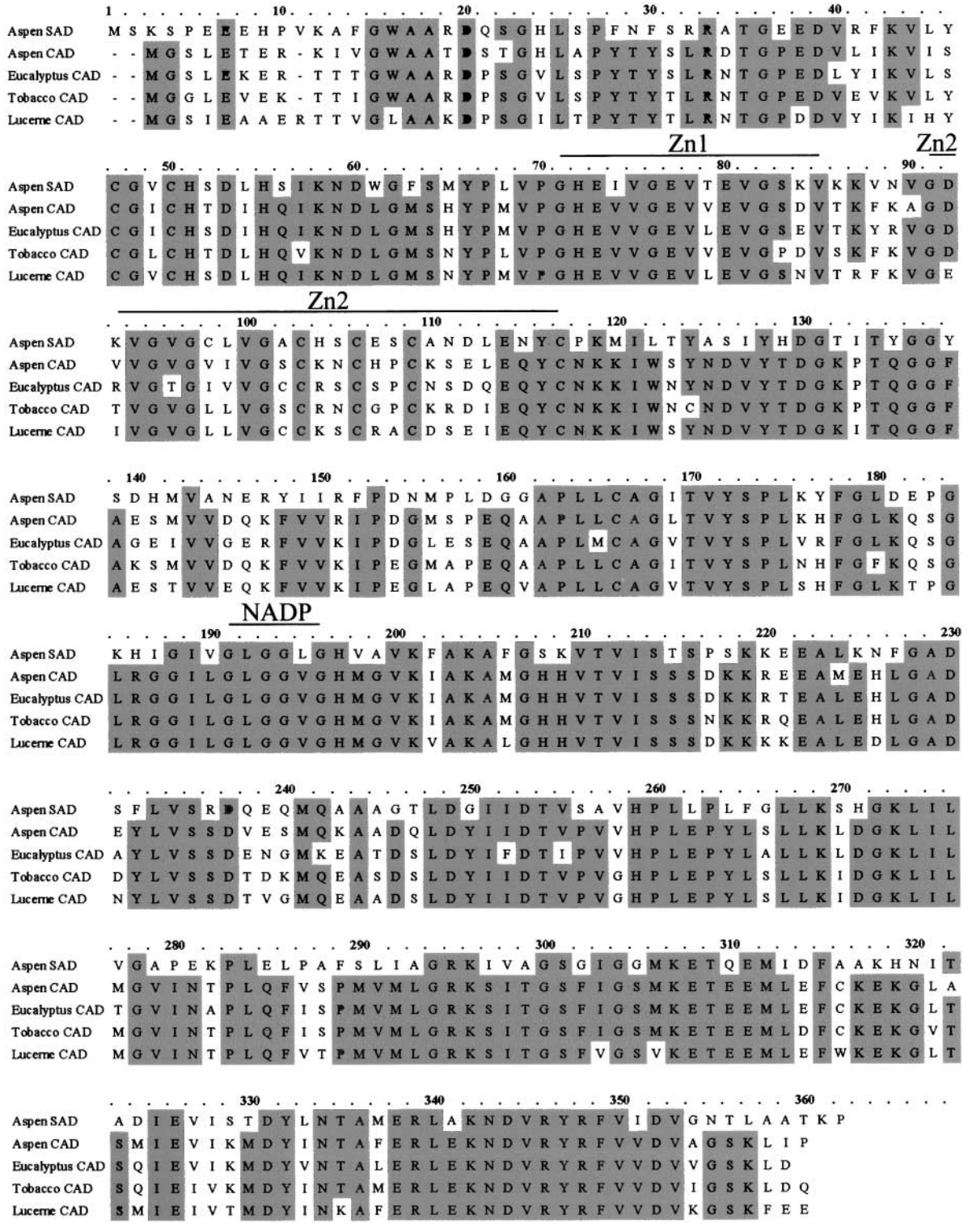


**Figure 1.** Amino Acid Sequence Alignment of Aspen SAD and Selected CAD Proteins.

The deduced amino acid sequences of aspen SAD and CAD, Eucalyptus CAD (*Eucalyptus globulus*), tobacco CAD (*Nicotiana tabacum*), and lucerne CAD (*Medicago sativa*) were aligned using the OMIGA program of the GCG software package (Genetics Computer Group, Madison, WI). Identical amino acid sequences are shaded. Locations of Zn1, Zn2, and NADP binding domains are indicated.

in $A_{340}$ attributable to the oxidation of NADPH, presumably coupled exclusively with the reduction of the aldehyde substrate provided (Wyrambik and Grisebach, 1975). The identities and quantities of all possible reduction products, including those of the alcohol product in question, can only be assumed. In this study, we developed an HPLC-UV/mass spectrometry (MS) approach to unambiguously quantify the authentic reaction products in all enzyme reactions. After reaction termination, the mixture was subjected directly to HPLC separation, and the structural identities and quantities of the separated reaction products were corroborated on the basis of diode array UV and MS signature comparisons with authentic compounds.

Using this HPLC-UV/MS system, we determined the functions of PtCAD and PtSAD by first testing the substrate specificity of the purified PtCAD and PtSAD recombinant proteins with various benzaldehyde and *p*-coumaraldehyde derivatives. PtCAD and PtSAD were inactive with benzaldehyde, 2-hydroxybenzaldehyde, *p*-hydroxybenzaldehyde, 3,4-dihydroxybenzaldehyde, vanillin, 5-hydroxyvanillin, and 5-methoxyvanillin but exhibited low or insignificant activity with 2-methoxybenzaldehyde and 3-methoxybenzaldehyde (data not shown). Preliminary results also showed that in sharp contrast, PtCAD and PtSAD exhibited high activities with all *p*-coumaraldehyde derivatives tested, PtSAD having the greatest activity with sinapaldehyde and PtCAD having the greatest activity with coniferaldehyde. Figures 4A and 4B show the typical HPLC-UV/MS results of PtCAD and PtSAD reactions with coniferaldehyde and sinapaldehyde, respectively. These aldehydes and their alcohol derivatives then were used as substrates to characterize the pH dependence of the PtCAD and PtSAD reduction and oxidation reactions (data not shown). Kinetic analyses of PtCAD- and PtSAD-catalyzed reductive reactions with *p*-coumaraldehyde derivatives then were conducted at their respective enzyme pH optima.

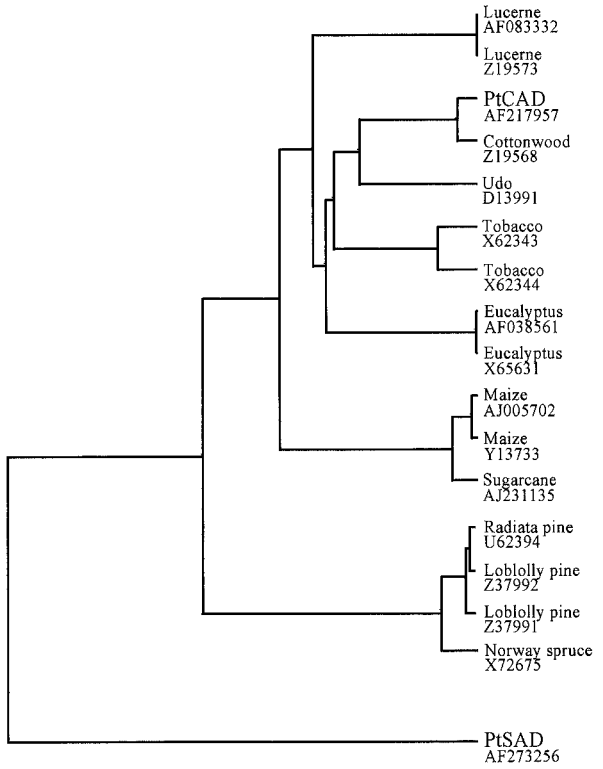


**Figure 2.** Phylogenetic Analysis of Aspen SAD and Plant CADs.

An unweighted pair-group method using arithmetic averages was used for phylogenetic tree analysis of aspen SAD (PtSAD) and other full-length plant CAD protein sequences available in the GenBank database.

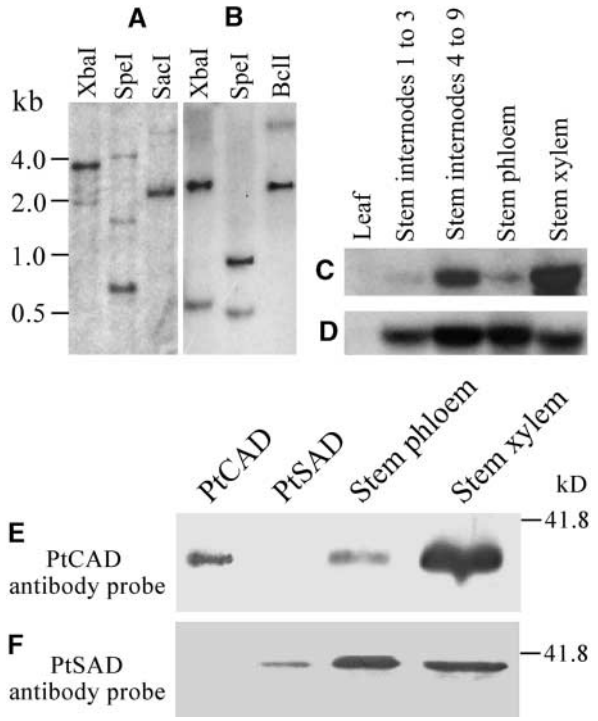


**Figure 3.** Molecular Characterization of Aspen *PtCAD* and *PtSAD*.

**(A)** and **(B)** Genomic DNA gel blot analysis. Aspen genomic DNA (10 μg/lane) was digested with restriction enzymes and hybridized with $^{32}$P-labeled full-length *PtCAD* **(A)** and *PtSAD* **(B)** cDNAs.

**(C)** and **(D)** RNA gel blot analysis of *PtCAD* and *PtSAD* tissue-specific expression patterns. Total RNA (10 μg/lane) from each organ or tissue type was hybridized with $^{32}$P-labeled full-length *PtCAD* **(C)** and *PtSAD* **(D)** cDNAs.

**(E)** and **(F)** Protein gel blot analysis of anti-PtCAD and anti-PtSAD antibody specificity and tissue-specific expression of PtCAD and PtSAD. Immunoblots of *E. coli*–expressed and affinity-purified PtCAD and PtSAD recombinant proteins (25 ng/lane) and plant protein extracts (10 μg/lane) with anti-PtCAD **(E)** and anti-PtSAD **(F)** antibodies.

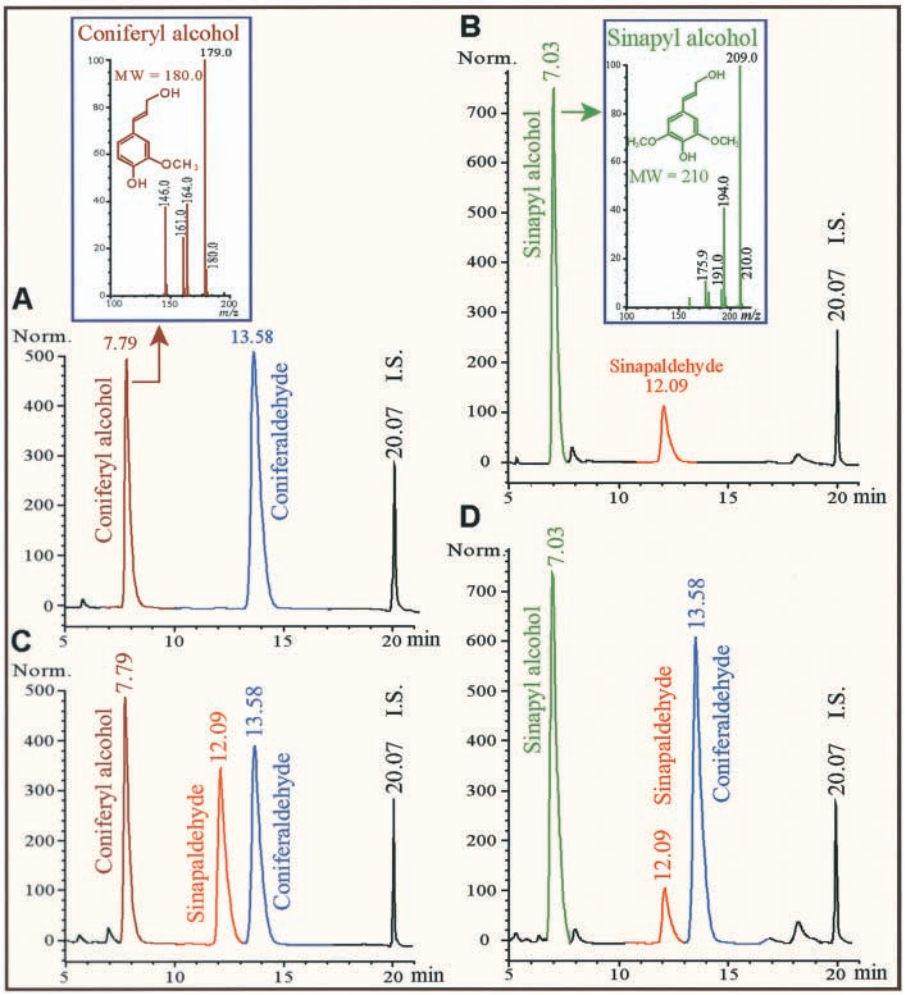


**Figure 4.** HPLC-UV/MS Analysis of Recombinant PtCAD and PtSAD Reactions.

**(A)** HPLC-MS (selected ion monitoring, 70 V; mass-to-charge ratio [*m/z*], 179.0) chromatogram showing the PtCAD reduction (see Methods) of coniferaldehyde (blue; retention time [Rt] = 13.58 min) into coniferyl alcohol (brown; Rt = 7.79 min). The inset shows the negative ion electrospray mass spectrum (scanning mode at 70 V) of coniferyl alcohol with properties (UV [HPLC mobile phase] $\lambda_{max}$ I, 262 nm, $\lambda_{max}$ II, 294 nm; MS [150 V] mass-to-charge ratio [%], 179.1 [100%], 164 [39%], 146 [38%], 161 [25%]) identical to the authentic standard. MW, molecular weight.
**(B)** HPLC-MS (selected ion monitoring, 70 V; mass-to-charge ratio [*m/z*], 209.0) chromatogram showing the PtSAD-mediated sinapaldehyde (red; Rt = 12.09 min) reduction (see Methods) into sinapyl alcohol (green; Rt = 7.03 min). The inset shows the negative ion electrospray mass spectrum of sinapyl alcohol with properties (UV [HPLC mobile phase] $\lambda_{max}$ I, 222 nm, $\lambda_{max}$ II, 274; MS [150 V] mass-to-charge ratio [%], 209.1 [100%], 194 [41%], 176 [11%]) identical to the authentic compound. MW, molecular weight.
**(C)** and **(D)** HPLC-MS (selected ion monitoring, 70 V; mass-to-charge ratio [*m/z*], 179.0 and 209.0) chromatograms of PtCAD and PtSAD reactions (see Methods) with a mixture of equal molar coniferaldehyde (blue; Rt = 13.58 min) and sinapaldehyde (red; Rt = 12.09 min). Coniferyl alcohol (brown; Rt = 7.79 min) is the exclusive product of the PtCAD reaction **(C)**, and sinapyl alcohol (green; Rt = 7.03 min) is the only product of the PtSAD reaction **(D)**.
*O*-Coumaric acid was the internal standard (I.S.) in all reactions.

## PtCAD and PtSAD Enzyme Kinetic Properties and Inhibition Kinetics

Lineweaver-Burk analysis (Tables 1 and 2) revealed significantly greater turnover rates for PtSAD-catalyzed reactions than for PtCAD-catalyzed reactions with all aldehydes tested. $V_{max}/K_m$ values demonstrated that coniferaldehyde was the preferred substrate for PtCAD and that the preferred PtSAD substrate was sinapaldehyde. In light of the increasing evidence that competition among structurally

similar monolignol pathway intermediates as substrates can modulate enzyme activities to affect phenolic metabolism (Osakabe et al., 1999; Li et al., 2000), we tested PtCAD and PtSAD in mixed substrate reactions. When a mixture of equal molar coniferaldehyde and sinapaldehyde was incubated with PtCAD, coniferaldehyde was converted into the guaiacyl monolignol, coniferyl alcohol, but sinapaldehyde reduction was blocked (Figure 4C). These findings provide evidence that CAD is guaiacyl specific and that a discrete SAD function is needed for the biosynthesis of syringyl monolignol. PtSAD would fulfill such a need, because it mediated the exclusive production of sinapyl alcohol from a mixture of coniferaldehyde and sinapaldehyde (Figure 4D). Evidently, sinapaldehyde also acted as an inhibitor of PtSAD-catalyzed coniferaldehyde reduction. To understand how coniferaldehyde may inhibit PtCAD-catalyzed sinapaldehyde reduction and how sinapaldehyde may block PtSAD-mediated coniferaldehyde reduction in vivo, we studied enzyme inhibition kinetics.

For both PtCAD and PtSAD proteins, the two-substrate interactions were of the competitive inhibition type (Figure 5). Coniferaldehyde, the preferred substrate of PtCAD, was a competitive inhibitor of PtCAD-catalyzed reduction of sinapaldehyde, with an apparent inhibition constant ($K_i$) of 1.7 μM (Figure 5A, inset), a value that was significantly lower than the $K_m$ (Table 1) of coniferaldehyde as a PtCAD substrate. Sinapaldehyde, the preferred PtSAD substrate, strongly inhibited PtSAD utilization of coniferaldehyde, with a $K_i$ of 0.5 μM (Figure 5B, inset), nearly 15 times lower than the $K_m$ (Table 2) of sinapaldehyde as a PtSAD substrate. These results provide evidence that in the presence of coniferaldehyde, PtCAD-mediated sinapaldehyde reduction is unlikely, and that in the presence of sinapaldehyde, PtSAD-catalyzed coniferaldehyde reduction would not take place in vivo. Thus, PtCAD is a coniferaldehyde- or guaiacyl-specific CAD and PtSAD is a sinapaldehyde- or syringyl-specific SAD. These results challenge the traditional model of monolignol biosynthesis and suggest that CAD mediates the reduction of coniferaldehyde into guaiacyl monolignol and that SAD along with CAld5H/AldOMT controls the biosynthesis and utilization of sinapaldehyde for syringyl monolignol.

### Histochemical and Chemical Detection of Guaiacyl and Syringyl Lignin Distributions in Aspen Stem Vascular Tissues

We began to identify the in situ relationship between PtCAD and PtSAD and guaiacyl and syringyl lignin biosynthesis by analyzing the distribution of guaiacyl and syringyl lignins in vascular systems of the aspen stem. Syringyl lignin can be distinguished chromogenically from guaiacyl lignin in situ by Cross/Bevan or Mäule color reaction (Nakano and Meshitsuka, 1992). The lignin-based chromophore-forming mechanisms in these two methods are similar. The chlorination of the syringyl nucleus leads to a pink (lignifying cells) or red (lignified cells) color, whereas the guaiacyl nucleus produces a light (lignifying cells) to dark (lignified cells) brown color (Bland, 1966; Wardrop, 1981). In this study, we used the Cross/Bevan method because of its mild reaction conditions, circumventing the problem of thin tissue section destruction that often occurs during Mäule color reactions.

In the primary vascular tissues, lignin was observed only in xylem and was of the guaiacyl type, as revealed by the brown staining of protoxylem and metaxylem vessel elements between stem internodes 1 and 4 (Figures 6A and 6B). This was further confirmed by thioacidolysis analysis of stem lignin, which demonstrated the exclusive detection of guaiacyl monomers (Figure 6D). The primary xylem remained as the only stem tissue containing pure guaiacyl lignin (Figures 6E to 6G). Guaiacyl-syringyl lignin appeared during the differentiation of secondary vascular systems, as indicated by the chemical analyses of stem internodes 5 and beyond (Figure 6H). However, the deposition of syringyl lignin in the secondary xylem followed that of guaiacyl lignin, as manifested by the color change from bright light brown to pink and then red in developing, partially lignified, and extensively lignified secondary xylem elements, respectively (Figure 6G). This is consistent with the reported sequential deposition of guaiacyl followed by syringyl lignins in xylem cells of angiosperms (Terashima et al., 1986; Saka and Goring, 1988).

Aggregated protophloem parenchyma cells, the precursors of primary phloem fibers (Esau, 1965), were present in

**Table 1.** Kinetic Properties of the Recombinant PtCAD Protein[a]

| Substrate | $K_m$ (μM) | $V_{max}$ (nmol·min$^{-1}$·μg$^{-1}$) | $k_{cat}$[b] (min$^{-1}$) | $V_{max}/K_m$ (%) |
|---|---|---|---|---|
| *p*-Coumaraldehyde | 6.2 ± 1.1 | 0.17 ± 0.04 | 6.8 ± 0.2 | 30.1 |
| Caffealdehyde | 37.0 ± 5.4 | 0.15 ± 0.03 | 6.0 ± 0.2 | 4.4 |
| Coniferaldehyde | 2.3 ± 0.8 | 0.21 ± 0.03 | 8.4 ± 0.3 | 100 |
| 5-Hydroxyconiferaldehyde | 17.5 ± 2.5 | 0.17 ± 0.04 | 6.8 ± 0.4 | 10.6 |
| Sinapaldehyde | 9.1 ± 1.2 | 0.10 ± 0.01 | 4.0 ± 0.2 | 12.0 |

[a] Values are means ±SE for three independent assays.
[b] $k_{cat}$, enzyme turnover number.

**Table 2.** Kinetic Properties of the Recombinant PtSAD Protein[a]

| Substrate | $K_m$ (μM) | $V_{max}$ (nmol·min$^{-1}$·μg$^{-1}$) | $k_{cat}$[b] (min$^{-1}$) | $V_{max}/K_m$ (%) |
|---|---|---|---|---|
| *p*-Coumaraldehyde | 15.6 ± 1.4 | 2.9 ± 0.3 | 116 ± 11 | 27.4 |
| Caffealdehyde | 140.0 ± 9.1 | 2.0 ± 0.1 | 80 ± 4 | 2.2 |
| Coniferaldehyde | 12.7 ± 1.5 | 2.3 ± 0.2 | 92 ± 6 | 26.6 |
| 5-Hydroxyconiferaldehyde | 36.1 ± 2.3 | 3.8 ± 0.4 | 152 ± 16 | 15.5 |
| Sinapaldehyde | 7.4 ± 1.1 | 5.0 ± 0.3 | 200 ± 13 | 100 |

[a] Values are means ±SE for three independent assays.
[b] $k_{cat}$, enzyme turnover number.

primary growth tissues (Figures 6A to 6C), but these cells were not stained for lignin, likely because of their lack of secondary wall thickening. They also failed to stain for guaiacyl lignin once lignification and secondary thickening began (Figure 6I). Instead, syringyl-positive pink (Figure 6I) to red (Figures 6E and 6F) coloration prevailed in these cells as they differentiated into fibers. Indeed, phloem fibers are known for their enrichment in syringyl lignin, but they do accumulate guaiacyl-syringyl lignin (Grand et al., 1982). Together, these observations indicate that in direct contrast to the lignification sequence in secondary xylem elements, the biosynthesis of syringyl lignin precedes and overwhelms that of guaiacyl lignin in primary phloem fibers.

We then used immunolocalization to verify whether PtCAD is associated with guaiacyl lignin–synthesizing primary xylem and whether the distribution of PtCAD and PtSAD is in line with the guaiacyl and syringyl lignin deposition patterns in phloem and xylem elements. The distribution of another syringyl pathway protein, PtCAld5H, also was analyzed.

### Immunolocalization of PtCAD, PtCAld5H, and PtSAD in Aspen Stem Internodes

Conditions similar to those present during protein gel blot analyses, by which the specificities of PtCAD and PtSAD antibodies were verified (Figures 3E and 3F), were applied to cellular immunolocalization. PtSAD and PtCAld5H were visualized in tissue sections after the anti-rabbit IgG–alkaline phosphatase reaction with nitroblue tetrazolium/5-bromo-4-chloro-3-indolyl phosphate substrate. PtCAD signals were visualized with Fast Red substrate. Serial sections were analyzed. Preimmune serum used at the same protein concentration as the anti-PtCAD, anti-PtSAD, or anti-PtCAld5H antiserum gave no immunolabeling signal (data not shown). At the third internode, PtCAD was detected almost exclusively in developing metaxylem vessels (Figure 7A). PtSAD was not detected in metaxylem vessels but was most conspicuous in protophloem parenchyma cells and in the parenchymatous storage tissue, the medullary sheath (Figure 7B).

The cellular distribution of PtCAld5H (Figure 7C) conformed with that of PtSAD. At the third internode, the lignification and secondary wall thickening had begun in metaxylem vessels but not in protophloem parenchyma cells (Figures 6A to 6C). Consistently, no lignin color reaction was observed in protophloem parenchyma cells (Figure 6A), despite the detection in these cells of PtSAD and CAld5H (Figures 7B and 7C). However, at internode 6, both syringyl lignin deposition (Figure 6I) and PtSAD signals (data not shown) were observed in these cells undergoing differentiation into primary phloem fibers. At the eighth internode, PtSAD signals diminished in these differentiating fiber cells (Figure 7E), signifying the near completion of syringyl monolignol biosynthesis in these cells (Figure 6E).

At this stage, PtCAD became more conspicuous than PtSAD in these maturing fibers (Figure 7D), indicative of an active biosynthesis of guaiacyl monolignol. As the primary phloem continued its centripetal course of differentiation, new protophloem parenchyma cells appeared adjacent to the maturing fibers toward the center of the stem. These new primary phloem fiber precursors (Esau, 1965) were labeled with PtSAD (Figure 7E) but not yet with PtCAD (Figure 7D). At internode 12, PtSAD signals disappeared in primary phloem fibers (Figure 7I), suggesting the completion of syringyl monolignol biosynthesis in these cells. However, PtCAD signals remained strong in these maturing fibers (Figure 7H). At internode 15, neither PtCAD nor PtSAD was detected in these fibers that became fully lignified (data not shown). These results agree with those of histochemical lignin localization indicating that the biosynthesis of syringyl lignin precedes that of guaiacyl lignin in primary phloem fibers.

However, these procambium-derived primary phloem elements and the secondary xylem exhibited contrasting lignification sequences. PtCAD appeared in xylem fusiform initials before PtSAD (Figures 7H and 7I), consistent with chemical and histochemical evidence that the biosynthesis of syringyl lignin lags behind that of guaiacyl lignin in the secondary xylem. Furthermore, in the differentiating secondary xylem, PtCAD signals were most conspicuous in maturing vessels (Figures 7F and 7H) but also were strong in developing fiber and ray cells. PtSAD signals were strongest in syringyl lignin–enriched radial and axial ray cells (Figure 7G) (Wardrop and Dadswell, 1952; Musha and Goring, 1975) and were conspicuous in maturing fiber cells but were nearly absent

from developing vessels (Figures 7G and 7I). These protein distribution patterns in the secondary xylem were sustained through older internodes (data not shown). These results and histochemical observations consistently demonstrated that PtCAD is associated with cells specializing in guaiacyl lignin synthesis and that PtSAD and PtCAld5H are associated with vascular elements containing enriched syringyl lignin.

### Detection of CAD and SAD Proteins in Various Angiosperms

Protein gel blot analysis of stem xylem proteins from six angiosperms and one gymnosperm (Figure 8) indicated that CAD and SAD proteins likely are common to angiosperms. Only the CAD signal was detected for loblolly pine, a gymnosperm.

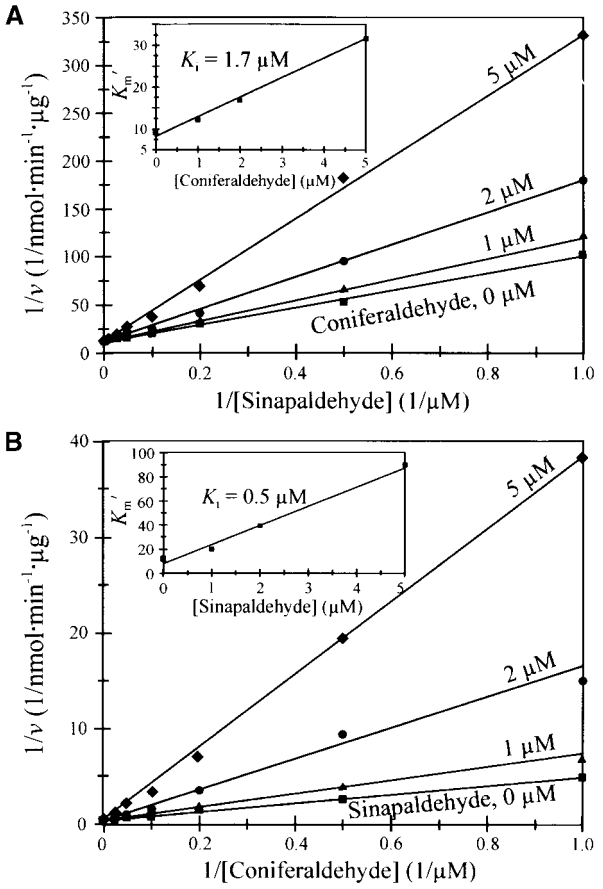


**Figure 5.** Inhibition Kinetics of PtCAD and PtSAD.

Lineweaver-Burk plots of 1/*v* versus 1/[S] in the presence of different levels of inhibitor concentrations as indicated. The insets show replots of apparent $K_m'$ versus the corresponding inhibitor concentration, used to calculated the $K_i$.

**(A)** Competitive inhibition effects of coniferaldehyde on PtCAD reduction of sinapaldehyde in mixed substrate assays.

**(B)** Competitive inhibition effects of sinapaldehyde on PtSAD reduction of coniferaldehyde in mixed substrate assays.

## DISCUSSION

### Principal Metabolic Fluxes Involving SAD and CAD for Monolignol Biosynthesis in Angiosperms

Our previous enzyme kinetic studies demonstrated that the pathway from caffeate to sinapate via ferulate and 5-hydroxyferulate (Figure 9) is unlikely because of CAld5H/AldOMT-mediated biosynthesis of sinapaldehyde from coniferaldehyde (Osakabe et al., 1999; Li et al., 2000). Certain recently published transgenic results confirmed our finding that caffeate methylation into ferulate is unlikely to occur in vivo during monolignol biosynthesis (Guo et al., 2001). We also had concluded that as a result of inhibiting the ferulate pathway, the 4-coumarate:CoA ligase (4CL)–catalyzed CoA ligation of sinapate, ferulate, and 5-hydroxyferulate would be obviated as paths to monolignols in vivo (Osakabe et al., 1999; Li et al., 2000).

Consistent with this conclusion, HPLC/MS analysis of the activity of aspen lignin–specific 4CL, Pt4CL1 (Hu et al., 1998, 1999), in mixed substrate assays showed that caffeate strongly inhibited the Pt4CL1-mediated CoA ligation of ferulate and *p*-coumarate (S.A. Harding, J. Leshkevich, V.L. Chiang, and C.J. Tsai, unpublished data). These results suggest a feedback mechanism by which any increase in levels of caffeate attributable to a CAld5H/AldOMT-modulated partial block of its methylation to ferulate would direct a phenolic flux through caffeate instead of through *p*-coumarate, caffeate, ferulate, 5-hydroxyferulate, or sinapate, as has been believed (Hahlbrock and Scheel, 1989; Whetten et al., 1998). This pathway intermediate–modulated feedback control lends support to a simple yet well-defined major phenolic flux to the biosynthesis of monolignols, a model we now propose (Figure 9, blue and red pathways).

The proposed principal flux through caffeate is consistent with the fact that caffeoyl-CoA, the predominant 4CL reaction product, also is the preferred substrate of caffeoyl-CoA *O*-methyltransferase for the biosynthesis of feruloyl-CoA (Ye et al., 1994; Zhong et al., 1998; Li et al., 1999), which in turn can be reduced in sequence most efficiently by cinnamoyl-CoA reductase (Lüderitz and Grisebach, 1981; Sarni et al., 1984; Goffner et al., 1994; Lacombe et al., 1997) and CAD (Figure 4C, Table 1) into the guaiacyl monolignol, coniferyl alcohol.

When intermediates (feruloyl-CoA, coniferaldehyde, and coniferyl alcohol) of the guaiacyl monolignol flux were reacted with angiosperm xylem protein extracts or CAld5H and AldOMT recombinant proteins, sinapaldehyde was the exclusive product, supporting the existence in angiosperms of a branch from the guaiacyl pathway at coniferaldehyde

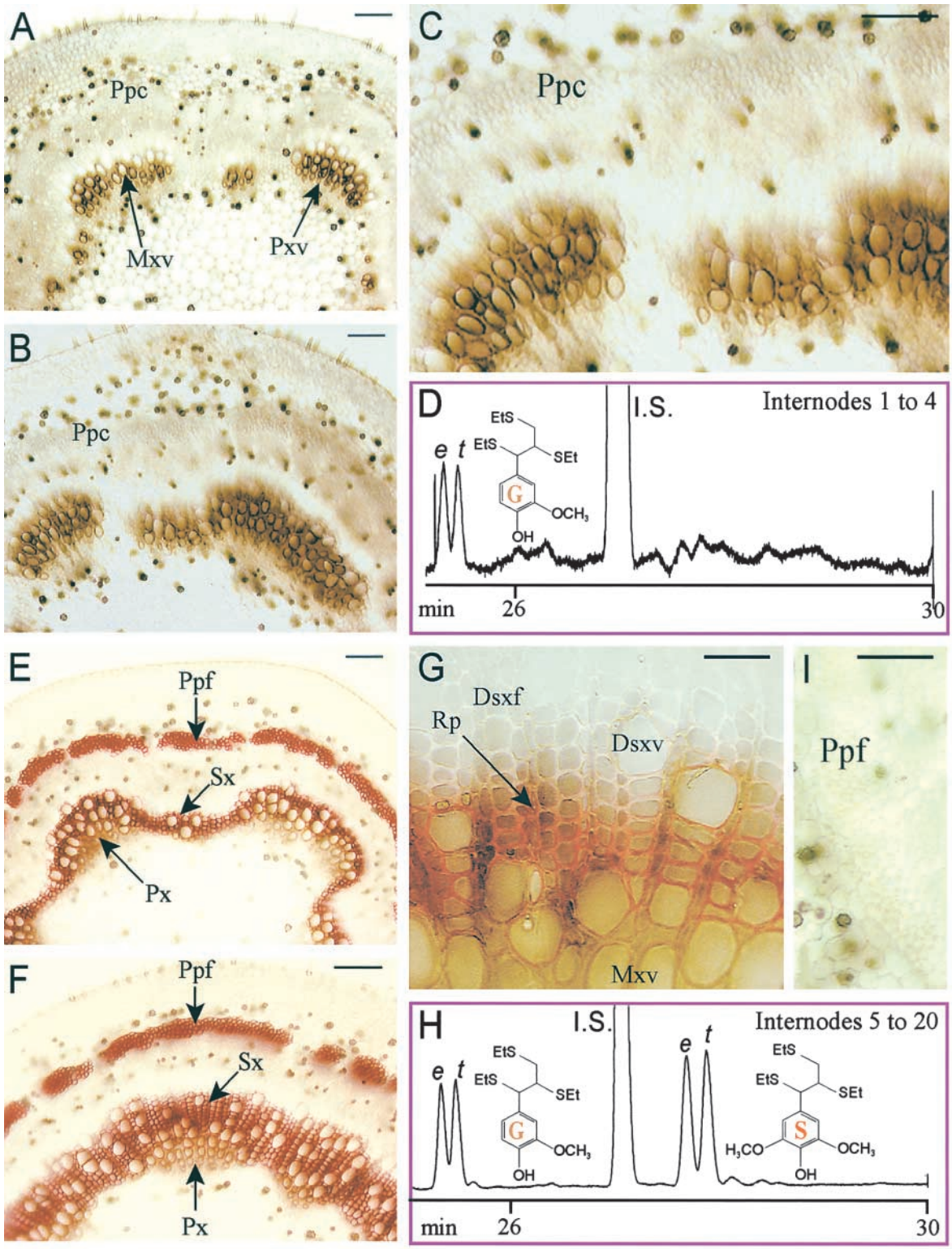


**Figure 6.** Detection of Guaiacyl and Syringyl Lignins in Aspen Stem.

Cross/Bevan histochemical analysis of transverse sections of stem internodes showing the exclusive presence of guaiacyl lignin (brown) in pri-

toward syringyl monolignol biosynthesis via sinapaldehyde (Osakabe et al., 1999; Li et al., 2000). We now report the discovery of a novel gene, *PtSAD*, encoding SAD, that together with CAld5H/AldOMT regulates the biosynthesis and utilization of sinapaldehyde for syringyl monolignol (Figure 9). Like the CAld5H/AldOMT-mediated initiation of the syringyl pathway (Li et al., 2000), SAD is widely distributed in angiosperms (Figure 8). Thus, the current results reinforce the model of a CAld5H/AldOMT/SAD pathway in common angiosperms for synthesizing syringyl monolignol and challenge the dated concept that CAD regulates the biosynthesis of both guaiacyl and syringyl monolignols.

With respect to the guaiacyl pathway (Figure 9), a shunt was suggested recently (Guo et al., 2001; Parvathi et al., 2001) in which caffeoyl-CoA, the most efficient caffeoyl-CoA *O*-methyltransferase substrate, is not methylated to feruloyl-CoA but instead is used by cinnamoyl-CoA reductase followed by CAD for the biosynthesis of caffealdehyde and caffeyl alcohol, respectively. However, the facts that caffeoyl-CoA is a poor cinnamoyl-CoA reductase substrate (Wengenmayer et al., 1976; Gross, 1980; Lüderitz and Grisebach, 1981) and that caffealdehyde is a poor substrate for both PtCAD and PtSAD (Tables 1 and 2), yielding no caffeyl alcohol in PtCAD or PtSAD reactions with mixed cinnamaldehyde derivatives, do not support the idea of such a shunt. Our previous (Zhang and Chiang, 1997; Osakabe et al., 1999; Li et al., 2000) and current results have consistently demonstrated mechanisms by which proteins with apparent broad substrate specificities may exhibit limited or directed functions as a result of substrate pool composition. Another substrate level–controlled reaction is the coniferaldehyde-modulated block of coniferyl alcohol 5-hydroxylation (Li et al., 2000), which negates a path from coniferyl alcohol to sinapyl alcohol previously proposed on the basis of isotope tracer studies (Chen et al., 1999).

However, other evidence from these tracer studies, such as the fact that the CAD-catalyzed oxidation of coniferyl alcohol to coniferaldehyde would lead to the biosynthesis of sinapyl alcohol via 5-hydroxyconiferaldehyde, is consistent with our model of syringyl monolignol biosynthesis. It also is consistent with biochemical demonstrations that the PtCAD-catalyzed oxidation of coniferyl alcohol exhibited significantly higher reaction rates in a wide pH range than the PtCAD-mediated coniferaldehyde reduction (data not shown). Thus, these in vivo and in vitro studies suggest that coniferyl alcohol is used not only for the biosynthesis of guaiacyl lignin but also for that of coniferaldehyde, supplementing the substrate pool for syringyl monolignol biosynthesis via CAld5H/AldOMT/SAD mediation. Together, this and the rapid PtSAD-mediated sinapaldehyde reduction would allow an efficient biosynthesis of syringyl lignin, the cell-strengthening component. Thus, the operation of a streamlined principal phenolic flux (Figure 9, blue and red pathways) would seem appropriate in vascular cells, which require timely lignification for basic structural and conducting functions to sustain tree growth and development.

### PtCAD and PtSAD Are Linked Spatiotemporally to the Differential Biosynthesis of Guaiacyl and Syringyl Lignins, Respectively, in Vascular Elements

In the primary xylem of aspen stem, only guaiacyl lignin is deposited (Figures 6A to 6D). No syringyl monolignol pathway proteins were detected in lignifying cells in this tissue. However, strong PtCAD signals were found in protoxylem and metaxylem vessel elements (Figure 7A), validating the idea that PtCAD is guaiacyl specific. PtCAld5H (Figure 7C), PtAldOMT (data not shown), and PtSAD (Figure 7B) were colocalized to protophloem parenchyma cells that would later

**Figure 6.** (continued).

mary xylem tissues (**[A]** to **[C]**) and the deposition of guaiacyl-syringyl lignin (red) in secondary growth tissues (**[E]** to **[G]** and **[I]**). The differential deposition of these lignins along the stem was confirmed by thioacidolysis analysis of the stem lignin (**[D]** and **[H]**).

**(A)** Internode 3.

**(B)** Internode 4.

**(C)** A magnified section of the image in **(B)**.

**(D)** and **(H)** Gas chromatograms of trithioethylated monomeric lignin products after thioacidolysis, demonstrating the exclusive presence of guaiacyl lignin in internodes 1 to 4 **(D)** and the presence of guaiacyl and syringyl lignins in internodes 5 to 20 **(H)**. Typical *erythro* (*e*) and *threo* (*t*) isomers (1:1 ratio) of guaiacyl and syringyl monomers were present. The internal standard (I.S.) was hexacosane.

**(E)** Internode 8. The primary xylem is the only vascular tissue having the pure guaiacyl lignin.

**(F)** Internode 10. The primary xylem is the only vascular tissue having the pure guaiacyl lignin.

**(G)** Internode 8 revealing the sequential deposition of guaiacyl (light brown) followed by syringyl (pink to red) lignins in secondary xylem elements. Note the deposition of only the guaiacyl lignin in metaxylem vessels.

**(I)** Internode 6 showing the onset of syringyl lignin (pink) deposition in primary phloem fibers.

Dsxf, developing secondary xylem fibers; Dsxv, developing secondary xylem vessels; Mxv, metaxylem vessels; Ppc, protophloem parenchyma cells; Ppf, primary phloem fibers; Px, primary xylem; Pxv, protoxylem vessels; Rp, ray parenchyma cells; Sx, secondary xylem. Bars in **(A)**, **(B)**, **(E)**, and **(F)** = 100 μm; bars in **(C)**, **(G)**, and **(I)** = 30 μm.

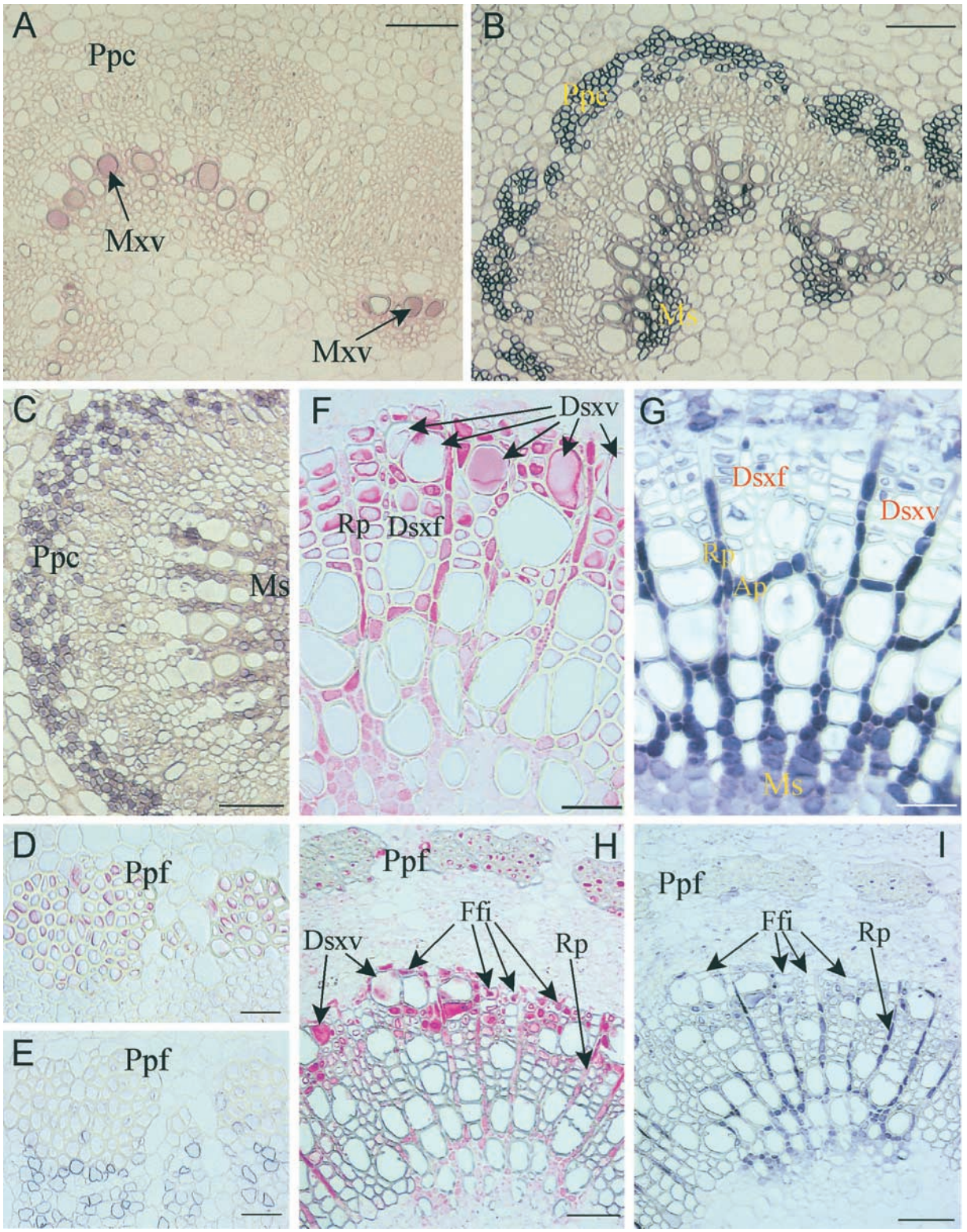


**Figure 7.** Immunolocalization of PtCAD, PtCAld5H, and PtSAD Proteins in Aspen Stem.

differentiate into syringyl lignin–enriched fibers (Figures 6E and 6F) (Grand et al., 1982). However, PtCAD was found in later differentiation stages of these fiber cells (Figures 7D and 7E), consistent with the fact that the biosynthesis of guaiacyl lignin lagged behind that of syringyl lignin in primary phloem fibers (Figures 6A, 6B, and 6I). These findings provide further evidence that PtCAD is guaiacyl specific and that PtSAD is syringyl specific. Moreover, the strong PtCAD signals (Figures 7F and 7H) and the near absence of PtSAD (Figures 7G and 7I) in secondary developing xylem vessels are consistent with the fact that vessels are enriched with the guaiacyl lignin (Fergus and Goring, 1970a, 1970b).

Both PtSAD and PtCAD are conspicuous in secondary developing xylem fiber cells, because these cells contain both syringyl and guaiacyl lignins (Musha and Goring, 1975; Saka and Goring, 1985) that likely originate from pools of sinapaldehyde and coniferaldehyde, respectively. In this case, the metabolic specificity of PtSAD and PtCAD would become modulated differentially by substrate pool composition. Although the precise cellular concentrations of these two aldehydes are unknown, we found that the total extractable sinapaldehyde and coniferaldehyde contents in developing aspen stem xylem cells were 110 and 12 ng/g fresh tissue, respectively, as quantified by HPLC/MS. In view of the fact that fiber elements constitute >80% of total vascular tissue volume (Fergus and Goring, 1970a, 1970b), the detected high sinapaldehyde/coniferaldehyde substrate pool ratios likely are typical in fiber cells. Thus, the enrichment of syringyl lignin in xylem fibers could be ascribed to the presence of PtSAD, because PtSAD would convert sinapaldehyde preferentially into syringyl monolignol according to substrate level–controlled kinetics (Figures 4 and 5).

One interesting observation was the conspicuous copresence of PtCAld5H, PtAldOMT, and PtSAD syringyl lignin proteins in ray parenchyma cells and particularly in the parenchymatous medullary zone (Figure 7). These cells are known for their storage function and may remain alive for many years (Frey-Wyssling and Bosshard, 1959; Esau, 1965), exporting cellular substances including proteins (Ryser and Keller, 1992). Thus, xylem radial and axial ray cells may serve as reservoirs that supply syringyl monolignol proteins to the adjacent fiber cells for syringyl lignin metabolism. This also may contribute to the high syringyl lignin content in xylem cells of heartwood formed after the autolysis of these cells (Kawamura and Higuchi, 1962). An enduring presence of syringyl monolignol proteins in ray cells and the medullary zone also suggests links to the biosynthesis of syringyl-type lignans during heartwood formation (Umezawa, 1994). Together, our results provide consistent evidence that guaiacyl-specific PtCAD and syringyl-specific PtSAD functions are linked spatiotemporally to the differential biosynthesis of guaiacyl and syringyl lignins and other specific monolignol-derived products in different cell types.

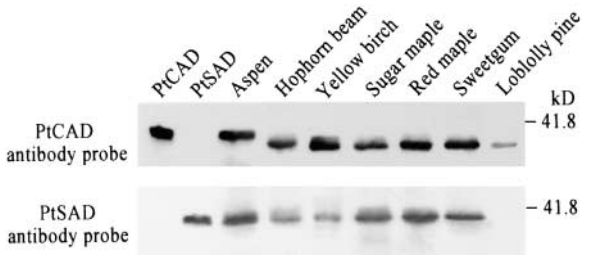


**Figure 8.** Immunoblot Detection of CAD and SAD Proteins in Various Plants.

CAD was detected by immunoblotting in developing xylem of all plants analyzed (top), but SAD was found only in angiosperm species (bottom). Seventy-five nanograms of recombinant protein per lane was used, and other lanes were loaded with 10 μg of plant xylem crude protein extracts.

## CAld5H/AldOMT/SAD Function Is Associated with Cell Support Function Specialization in Angiosperm Evolution

Lignin in the most primitive land plants, such as Psilopsida, is of the guaiacyl type (Wardrop, 1971). Its function in these plants was not so much in mechanical support but in conduction (Corner, 1968; Raven, 1977). The gymnosperms

**Figure 7.** (continued).

Light micrographs of stem transverse sections showing localizations of PtCAD (red; **[A]**, **[D]**, **[F]**, and **[H]**), PtCAld5H (blue; **[C]**), and PtSAD (blue; **[B]**, **[E]**, **[G]**, and **[I]**).

**(A)** to **(C)** Internode 3. PtCAD was localized exclusively to primary xylem elements **(A)**, whereas PtSAD **(B)** and PtCAld5H **(C)** were not detected in these primary xylem elements but were abundant in protophloem parenchyma cells and the medullary sheath.

**(D)** and **(E)** Primary phloem fibers in internode 8.

**(F)** and **(G)** Internode 8. Note the strong PtCAD signals in developing secondary xylem vessels **(F)**, but PtSAD signals were nearly absent from these cells **(G)**.

**(H)** and **(I)** Internode 12. The appearance of PtSAD **(I)** lagged behind that of PtCAD **(H)** in fusiform initials.

Ap, axial ray parenchyma cells; Ffi, fusiform initials; Ms, medullary sheath. Other abbreviations are as given in Figure 6. Bars in **(A)** to **(C)**, **(H)**, and **(I)** = 50 μm; bars in **(D)** to **(G)** = 30 μm.

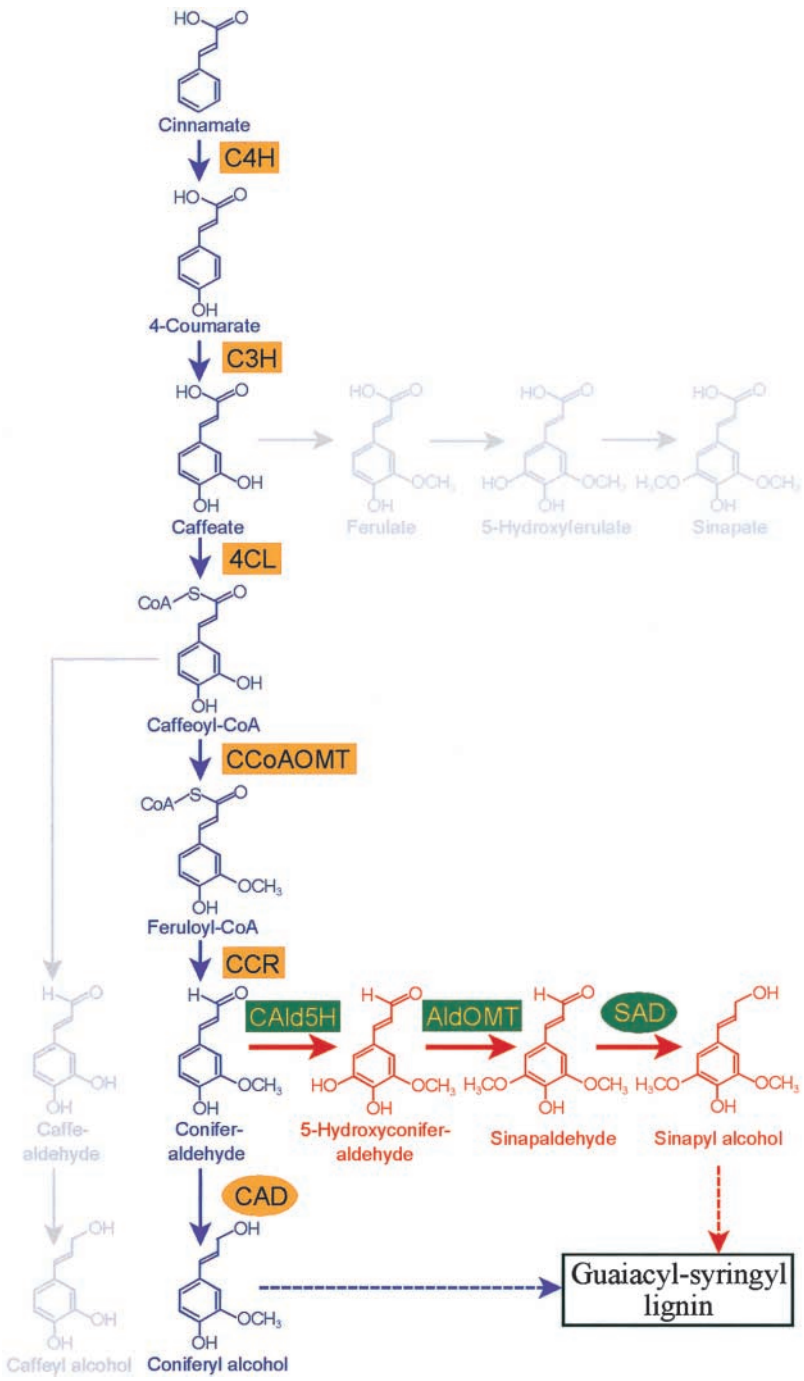


**Figure 9.** Proposed Principal Biosynthetic Pathway for the Formation of Monolignols in Angiosperms.

C4H, cinnamate 4-hydroxylase; C3H, 4-coumarate 3-hydroxylase; 4CL, 4-coumarate:CoA ligase; CCoAOMT, caffeoyl-CoA *O*-methyltransferase; CCR, cinnamoyl-CoA reductase. Inconclusive pathways are shown in gray.

of the Middle Devonian Period developed extensive secondary xylem consisting mainly of tracheids with dual functions in conduction and mechanical support (Wardrop, 1981). Interestingly, the gradual evolution of gymnosperms from ancient Devonian ferns was not accompanied by detectable changes in lignin structure (Sarkanen and Hergert, 1971).

Conceivably, the guaiacyl lignin always has been linked largely to conduction function. In angiosperm evolution, the functions of conduction and mechanical support were divided among vessels and xylem fibers, respectively, two specialized cell types that emerged from primitive tracheids (Esau, 1965). Thus, it is possible that the evolution of fiber cells concomitant with the emergence of syringyl lignin biosynthesis provided significant mechanical advantages to angiosperm species. Consistent with this view, "tension wood" produced specifically in angiosperm trees for corrective growth to counteract mechanical and gravitational stimuli develops an abnormally high frequency of fibers but relatively few vessels (Wardrop and Davies, 1964; Scurfield, 1973). These fibers are characterized by their exceptionally high syringyl lignin content compared with that of normal wood fibers (Sarkanen and Hergert, 1971). In contrast, the less rigid, so-called rubbery wood of apple trees has lignins that are scarcely methylated (Scurfield and Bland, 1963), a type that resembles guaiacyl lignin. This insufficiently methylated lignin is known for its vulnerability to Mycoplasma infection (Scurfield and Bland, 1963). Therefore, we suggest that mechanical support and pathogen resistance offer selection advantages that favor the evolution of CAld5H/AldOMT/SAD and the copolymerization of the guaiacyl-syringyl lignin in angiosperms.

In addition to the amenability of syringyl lignin to chemical extraction during cellulose-based wood processing for materials and chemicals, its unique growth-conducive mechanical and perhaps pathogen defense functions add further incentives to engineering such a lignin type in gymnosperms, which contain chemically resistant guaiacyl lignin but superior tracheid elements for paper/wood-related products. Therefore, our results, which add new mechanistic insights to the understanding of syringyl monolignol biosynthesis, may help facilitate such biotechnological endeavors (Trotter, 1990).

## METHODS

### Isolation of Aspen *SAD* cDNA

A randomly primed, $^{32}$P-labeled, full-length *PtCAD* cDNA probe (GenBank accession number AF217957) was used to screen an aspen (*Populus tremuloides*) stem developing xylem cDNA library (Wu et al., 2000) under high and low stringency conditions for cDNAs that were distinct from *PtCAD*. Four identical copies of plaque-forming units ($2.4 \times 10^4$) were hybridized with the probe, two under high stringency conditions (65°C) and the other two under low stringency conditions (50°C). Sequence analysis revealed that the positive clones that hybridized with the probe simultaneously under high and low stringency conditions had sequences identical to *PtCAD*. Sequences of clones that hybridized with the probe only under low stringency conditions were identical to each other but distinct from *PtCAD*. Two of these low stringency probe–hybridizing clones were found to be full-length cDNAs; they were designated *PtSAD* and sequenced (ABI310; Perkin-Elmer) in both directions (GenBank accession number AF273256).

### DNA and RNA Gel Blot Analysis

Aspen genomic DNA and total RNA from various aspen tissues were isolated as described (Li et al., 1997; Hu et al., 1998). DNA and RNA gel blot hybridizations were performed under high stringency conditions (Hu et al., 1998). Probes were *PtCAD* or *PtSAD* cDNA labeled with $\alpha$-$^{32}$P-dATP (Amersham) using the DECAprimeII labeling system (Ambion, Austin, TX).

### Expression and Purification of PtCAD and PtSAD Recombinant Proteins and Preparation of Plant Protein Extracts

The coding sequences of *PtCAD* and *PtSAD* were amplified by polymerase chain reaction (PCR) using primers designed to introduce NdeI and NotI sites immediately upstream of their start and stop codons. The PCR product was cloned into the NdeI and NotI sites of pET23 $b^+$ vector (Novagen, Madison, WI) to fuse a His tag at the C terminus of the cloned sequence. After sequence confirmation, the engineered pET23 $b^+$ construct was transferred into *Escherichia coli* host strain BL21(DE3) (Novagen). Induction and purification of recombinant PtCAD and PtSAD were performed as described (Li et al., 2000). Differentiating stem xylem was collected during the growing season from aspen, hophorn beam (*Ostrya virginiana*), yellow birch (*Betula alleghaniensis*), sugar maple (*Acer saccharum*), red maple (*Acer rubrum*), sweetgum (*Liquidambar styraciflua*), and loblolly pine (*Pinus taeda*) and used to isolate crude protein extracts as described (Li et al., 2000).

### Preparation of Anti-PtCAD and Anti-PtSAD Antibodies and Protein Gel Blot Analysis

The affinity-purified PtCAD and PtSAD recombinant proteins were used to immunize rabbits (Alpha Diagnostic, San Antonio, TX). The antibodies, diluted 1:3000, were used in protein gel blot analyses of xylem crude proteins (Osakabe et al., 1999). Protein concentrations were determined by the Bio-Rad protein assay system.

### Chemical Synthesis and Thioacidolysis Analysis of Aspen Stem Monolignol Composition

All aldehydes and their alcohol derivatives were obtained from Sigma/Aldrich, except the following. *p*-Coumaraldehyde, *p*-coumaryl alcohol, caffealdehyde, caffeyl alcohol, 5-hydroxyconiferaldehyde, and 5-hydroxyconiferyl alcohol were prepared chemically from their corresponding benzaldehyde derivatives as described (Osakabe et al., 1999; Li et al., 2000). The structural identities of these compounds were confirmed by $^1$H-NMR. *p*-Coumaraldehyde: $\delta$ (acetone-$d_6$; standard carbon numbers were used) 6.48 (1H, dd, $J1 = 15.9$, $J2 = 7.8$, $C_8$H), 6.80 (2H, m, Ar-H), 7.46 (1H, d, $J = 15.8$, $C_7$H), 7.48 (2H, m, Ar-H), 9.50 (1H, d, $C_9$H); *p*-coumaryl alcohol: $\delta$ (acetone-$d_6$) 4.18 (2H,

dd, *J1* = 4, *J2* = 1, $C_9H$), 6.19 (1H, dt, *J1* = 15.9, *J2* = 5.5, $C_8H$), 6.49 (1H, d, *J* = 15.9, $C_7H$), 6.78 (2H, m, Ar-H), 7.26 (2H, m, Ar-H); caffealdehyde: δ (acetone-$d_6$) 6.53 (1H, dd, *J1* = 15.7, *J2* = 7.6, $C_8H$), 6.90 (1H, d, *J* = 7.9, $C_5H$), 7.10 (1H, dd, *J1* = 7.9, *J2* = 2.1, $C_6H$), 7.20 (1H, d, *J* = 2.1, $C_2H$), 7.51 (1H, d, *J* = 15.7, $C_7H$), 9.61 (1H, d, *J* = 7.6, $C_9H$); caffeyl alcohol: δ (acetone-$d_6$) 4.17 (2H, d, *J* = 5.5, $C_9H$), 6.14 (1H, dt, *J1* = 15.9, *J2* = 5.5, $C_8H$), 6.43 (1H, dt, *J1* = 15.9, *J2* = 1.5, $C_7H$), 6.75 (2H, d, *J* = 1.5, $C_5H$, $C_6H$), 6.92 (1H, d, *J* = 1.5, $C_2H$); 5-hydroxyconiferaldehyde: δ (acetone-$d_6$) 3.88 (3H, s, $OCH_3$), 6.60 (1H, dd, *J1* = 15.6, *J2* = 7.8, $C_8H$), 6.88 (1H, d, *J* = 1.7, $C_6H$), 6.95 (1H, d, *J* = 1.7, $C_2H$), 7.50 (1H, d, *J* = 15.6, $C_7H$), 9.61 (1H, d, *J* = 7.8, $C_9H$); 5-hydroxyconiferyl alcohol: δ (acetone-$d_6$) 3.87 (3H, s, $OCH_3$), 4.28 (2H, t, *J* = 5.5, $C_9H$), 6.20 (1H, dt, *J1* = 15.9, *J2* = 5.5, $C_8H$), 6.47 (1H, d, *J* = 15.9, $C_7H$), 6.51 (1H, d, *J* = 1.8, $C_6H$), 6.64 (1H, d, *J* = 1.8, $C_2H$). For analysis of monolignol composition, aspen stem internodes were extracted with benzene/alcohol and subjected to gas chromatography–mass spectrometry (MS)-based thioacidolysis (Rolando et al., 1992; Tsai et al., 1998).

### HPLC-UV/MS Analysis of Enzyme Functions and Reaction Kinetics

The basic enzyme reaction mixture contained 50 mM sodium phosphate buffer, 5 mM β-mercaptoethanol, 500 μM NADPH or NADP, purified recombinant protein (boiled protein was used as a control), and phenolic substrate in a final volume of 500 μL. For the substrate specificity test, 500 μM aldehyde substrate and 1 μg of purified recombinant PtCAD or PtSAD protein (~25 pmol) were used. To characterize the enzyme pH optima, the substrate and recombinant PtCAD or PtSAD protein concentrations described above were used in sodium phosphate buffers, pH 5 to 8.5. All reactions were for 10 min at 30°C.

For normal and inhibition kinetic analyses, the reaction time was 4 min and pH was 8.0 for PtCAD (1.2 μg of purified recombinant protein) and 7.0 for PtSAD (0.1 μg). For kinetics, varying concentrations (0.5 to 200 μM) of *p*-coumaraldehyde, caffealdehyde, coniferaldehyde, 5-hydroxyconiferaldehyde, or sinapaldehyde were used to measure $K_m$, $V_{max}$, and the enzyme turnover number, $k_{cat}$. For inhibition kinetics, the PtCAD-mediated reduction of sinapaldehyde (1 to 200 μM) was assayed in the presence of 1 to 5 μM coniferaldehyde, and the PtSAD-catalyzed reduction of coniferaldehyde (1 to 200 μM) was assayed in the presence of 1 to 5 μM sinapaldehyde. All reactions were terminated by the addition of 10 μL of 6 N HCl (to bring the pH to 2) and 500 ng of internal standard *o*-coumaric acid and analyzed by HPLC-UV/MS.

An aliquot of 100 μL of reaction mixture was injected directly onto a Supelcosil LC-ABZ column (15 cm × 4.6 mm × 5 μm; Supelco, Bellefonte, PA) with automatic sample injection and separated isocratically with a Hewlett-Packard (HP) 1100 liquid chromatography system at 40°C and a flow rate of 0.25 mL/min. The gradient program was 20% acetonitrile in 10 mM formic acid, pH 2.5, for 12 min, 20 to 100% acetonitrile from 12 to 16 min, and hold at 100% acetonitrile for 5 to 10 min; detection was with an HP 1100 diode array detector and an HP 1100 liquid chromatography–MS detector system with an atmospheric pressure ionization–electrospray source in negative ion mode. The reaction products were identified and confirmed by comparing the ion fragmentation patterns of the product and the authentic standard in MS scanning mode at 70 V. The product quantity and $K_m$, $V_{max}$, $k_{cat}$, and apparent inhibition constant ($K_i$) values (means ±SE) were determined as described (Osakabe et al., 1999; Li et al., 2000).

### Histochemical Lignin Analysis, Immunolocalization, and Microscopy

For histochemical localization of lignin, fresh hand-cut sections (~20 μm thick) from stem internodes of 4-month-old, greenhouse-grown aspen plants (clone 271) were incubated immediately in freshly prepared saturated chlorinated water for 10 min at 4°C. After three washes with water, the sections were incubated in 4% sodium sulfite at room temperature for 5 min, mounted in 50% glycerol, and photographed using a Nikon (Tokyo, Japan) Eclipse 400 fluorescence microscope. Segments (~1 mm thick) from the same internodes used for histochemical analysis were used for immunolocalization on the basis of the protocol of Wittich et al. (1999) with modifications. The segments were fixed in 4% paraformaldehyde in 0.1 M PBS (4 mM sodium phosphate, pH 7.4, and 200 mM NaCl) for 12 hr at 4°C. After washing in PBS for 2 hr at 4°C, the segments were dehydrated in an ethanol series, infiltrated, and embedded in butyl methyl methacrylate.

Polymerization was performed under UV light (365 nm) for 40 hr at −20°C in a UVC2 CRYO Chamber (PELCO, Redding, CA). Sections (3 μm thick) were prepared with a Leica (Wetzlar, Germany) RM 2155 microtome and mounted on Superfrost/plus (Fisher) slides. Slides were rinsed with acetone to remove butyl methyl methacrylate from the sections, which were rehydrated in an ethanol series and blocked first with 0.1 M hydroxyammonium chloride for 5 min and then with 1% BSA for 30 min at room temperature. After incubation with anti-PtCAD, anti-PtCAld5H (Osakabe et al., 1999), anti-PtAldOMT (Li et al., 2000), or anti-PtSAD antibodies (in 1:500 dilution) for 2 hr at 37°C, slides were washed in PBS containing 0.1% BSA and incubated with goat anti-rabbit antibody conjugated with alkaline phosphatase (1:100; Boehringer Mannheim) for 1.5 hr at 37°C. After washing in PBS, slides incubated with anti-PtSAD, anti-PtCAld5H, or anti-PtAldOMT antibodies were reacted at pH 9.5 with a mixture of dimethylformamide and nitroblue tetrazolium/5-bromo-4-chloro-3-indolyl phosphate, and those incubated with anti-PtCAD antibodies were treated with Fast Red TR/Naphthol AS-MX (Sigma); both treatments were for 20 to 30 min at room temperature. Preimmune serum was used as the control. The slides then were mounted in 50% glycerol and observed with a Nikon Eclipse 400 microscope, and images were taken using a Sony (Tokyo, Japan) DKC-5000 digital photo camera.

### GenBank Accession Numbers

The GenBank accession numbers are as follows: aspen SAD AF273256; aspen CAD AF217957; *Eucalyptus globulus* AF038561; *Nicotiana tabacum* X62343; *Medicago sativa* AF083332.

### ACKNOWLEDGMENTS

We thank Shiro Suzuki (Kyoto University, Japan) for his contribution to this article. This work was supported by the Energy Biosciences Program, United States Department of Energy, and a Michigan Technological University, School of Forestry, research grant.

Received March 14, 2001; accepted May 12, 2001.

## REFERENCES


**Baucher, M., Chabbert, B., Pilate, G., Van Doorsselaere, J., Tollier, M.T., Petit-Conil, M., Monties, B., Van Montagu, M., Inzé, D., Jouanin, L., and Boerjan, W.** (1996). Red xylem and higher lignin extractability by down-regulating a cinnamyl alcohol dehydrogenase in poplar (*Populus tremula* × *Populus alba*). Plant Physiol. **112,** 1479–1490.

**Bland, D.E.** (1966). Colorimetric and chemical identification of lignins in different parts of *Eucalyptus botryoides* and their relation to lignification. Holzforschung **20,** 12–16.

**Boudet, A.M., Lapierre, C., and Grima-Pettenati, J.** (1995). Biochemistry and molecular biology of lignification. New Phytol. **129,** 203–226.

**Brill, E.M., Abrahams, S., Hayes, C.M., Jenkins, C.L.D., and Watson, J.M.** (1999). Molecular characterization and expression of a wound-inducible cDNA encoding a novel cinnamyl-alcohol dehydrogenase enzyme in lucerne. Plant Mol. Biol. **41,** 279–291.

**Chen, F., Yasuda, S., and Fukushima, K.** (1999). Evidence for a novel biosynthetic pathway that regulates the ratio of syringyl to guaiacyl residues in lignin in the differentiating xylem of *Magnolia kobus* DC. Planta **207,** 597–603.

**Corner, E.J.H.** (1968). The Life of Plants. (New York: New American Library).

**Esau, K.** (1965). Plant Anatomy, 2nd ed. (New York: John Wiley and Sons).

**Fergus, B.J., and Goring, D.A.I.** (1970a). The location of guaiacyl and syringyl lignins in birch xylem tissue. Holzforschung **24,** 113–117.

**Fergus, B.J., and Goring, D.A.I.** (1970b). The distribution of lignin in birch wood as determined by ultraviolet microscopy. Holzforschung **24,** 118–124.

**Frey-Wyssling, A., and Bosshard, H.H.** (1959). Cytology of the ray cells in sapwood and heartwood. Holzforschung **13,** 129–137.

**Galliano, H., Cabane, M., Eckerskorn, C., Lottspeich, F., Sandermann, H., and Ernst, D.** (1993a). Molecular cloning, sequence analysis and elicitor-/ozone-induced accumulation of cinnamyl alcohol dehydrogenase from Norway spruce (*Picea abies*). Plant Mol. Biol. **23,** 145–156.

**Galliano, H., Heller, W., and Sandermann, H., Jr.** (1993b). Ozone induction and purification of spruce cinnamyl alcohol dehydrogenase. Phytochemistry **32,** 557–563.

**Goffner, D., Joffroy, I., Grima-Pettenati, J., Halpin, C., Knight, M.E., Schuch, W., and Boudet, A.M.** (1992). Purification and characterization of isoforms of cinnamyl alcohol dehydrogenase from Eucalyptus xylem. Planta **188,** 48–53.

**Goffner, D., Campbell, M.M., Campargue, C., Clastre, M., Borderies, G., Boudet, A., and Boudet, A.M.** (1994). Purification and characterization of cinnamoyl-CoA:NADP oxidoreductase in *Eucalyptus gunnii*. Plant Physiol. **106,** 625–632.

**Goffner, D., Van Doorsselaere, J., Yahiaoui, N., Samaj, J., Grima-Pettenati, J., and Boudet, A.M.** (1998). A novel aromatic alcohol dehydrogenase in higher plants: Molecular cloning and expression. Plant Mol. Biol. **36,** 755–765.

**Grand, C., Boudet, A.M., and Ranjeva, R.** (1982). Natural variations and controlled changes in lignification process. Holzforschung **36,** 217–223.

**Grima-Pettenati, J., Feuillet, C., Goffner, D., Borderies, G., and Boudet, A.M.** (1993). Molecular cloning and expression of a *Eucalyptus gunnii* cDNA clone encoding cinnamyl alcohol dehydrogenase. Plant Mol. Biol. **21,** 1085–1095.

**Grima-Pettenati, J., Campargue, C., Boudet, A., and Boudet, A.M.** (1994). Purification and characterization of cinnamyl alcohol dehydrogenase isoforms from *Phaseolus vulgaris*. Phytochemistry **37,** 941–947.

**Gross, G.G.** (1980). The biochemistry of lignification. Adv. Bot. Res. **8,** 25–63.

**Guo, D., Chen, F., Inoue, K., Blount, J.W., and Dixon, R.A.** (2001). Downregulation of caffeic acid 3-*O*-methyltransferase and caffeoyl CoA 3-*O*-methyltransferase in transgenic alfalfa: Impacts on lignin structure and implications for the biosynthesis of G and S lignin. Plant Cell **13,** 73–88.

**Hahlbrock, K., and Scheel, D.** (1989). Physiology and molecular biology of phenylpropanoid metabolism. Annu. Rev. Plant Physiol. Plant Mol. Biol. **40,** 347–369.

**Halpin, C., Knight, M.E., Grima-Pettenati, J., Goffner, D., Boudet, A., and Schuch, W.** (1992). Purification and characterization of cinnamyl alcohol dehydrogenase from tobacco stems. Plant Physiol. **98,** 12–16.

**Halpin, C., Knight, M.E., Foxon, C.A., Campbell, M.M., Boudet, A.M., Boon, J.J., Tollier, M.T., and Schuch, W.** (1994). Manipulation of lignin quality by downregulation of cinnamyl alcohol dehydrogenase. Plant J. **6,** 339–350.

**Hawkins, S.E., and Boudet, A.M.** (1994). Purification and characterization of cinnamyl alcohol dehydrogenase isoforms from the periderm of *Eucalyptus gunnii* Hook. Plant Physiol. **104,** 75–84.

**Hibino, T., Shibata, D., Umezawa, T., and Higuchi, T.** (1993a). Purification and partial sequences of *Aralia cordata* cinnamyl alcohol dehydrogenase. Phytochemistry **32,** 565–567.

**Hibino, T., Shibata, D., Chen, J.-Q., and Higuchi, T.** (1993b). Cinnamyl alcohol dehydrogenase from *Aralia cordata*: Cloning of the cDNA and expression of the gene in lignified tissues. Plant Cell Physiol. **34,** 659–665.

**Higuchi, T.** (1997). Biochemistry and Molecular Biology of Wood. (New York: Springer-Verlag).

**Higuchi, T., Ito, T., Umezawa, T., Hibino, T., and Shibata, D.** (1994). Red-brown color of lignified tissues of transgenic plants with antisense CAD gene: Wine-red lignin from coniferyl aldehyde. J. Biotechnol. **37,** 151–158.

**Hu, W.-J., Kawaoka, A., Tsai, C.-J., Lung, J., Osakabe, K., Ebinuma, H., and Chiang, V.L.** (1998). Compartmentalized expression of two structurally and functionally distinct 4-coumaric acid:coenzyme A ligase (4CL) genes in aspen (*Populus tremuloides*). Proc. Natl. Acad. Sci. USA **95,** 5407–5412.

**Hu, W.-J., Lung, J., Harding, S.A., Popko, J.L., Ralph, J., Stokke, D.D., Tsai, C.-J., and Chiang, V.L.** (1999). Repression of lignin biosynthesis promotes cellulose accumulation and growth in transgenic trees. Nat. Biotechnol. **17,** 808–812.

**Humphreys, J.M., Hemm, M.R., and Chapple, C.** (1999). New routes for lignin biosynthesis defined by biochemical characterization of recombinant ferulate 5-hydroxylase, a multifunctional cytochrome P450-dependent monooxygenase. Proc. Natl. Acad. Sci. USA **96,** 10045–10050.

**Jornvall, H., Person, B., and Jeffery, J.** (1987). Characterization of alcohol/polyol dehydrogenases: The zinc-containing long chain alcohol dehydrogenases. Eur. J. Biochem. **167,** 195–201.

**Kawamura, I., and Higuchi, T.** (1962). Studies on the lignin of young tissues of wood. I. On lignin of *Pseudoacacia*. J. Jpn. Wood Res. Soc. **8,** 148–153.

**Knight, M.E., Halpin, C., and Schuch, W.** (1992). Identification and characterization of cDNA clones encoding cinnamyl alcohol dehydrogenase from tobacco. Plant Mol. Biol. **19,** 793–801.

**Kutsuki, H., Shimada, M., and Higuchi, T.** (1982). Regulatory role of cinnamyl alcohol dehydrogenase in the formation of guaiacyl and syringyl lignins. Phytochemistry **21,** 19–23.

**Lacombe, E., Hawkins, S., Doorsselaere, J.V., Piquemal, J., Goffner, D., Poeydomenge, O., and Boudet, A.M.** (1997). Cinnamoyl CoA reductase, the first committed enzyme of the lignin branch biosynthetic pathway: Cloning, expression and phylogenetic relationships. Plant J. **11,** 429–441.

**Li, L., Popko, J.L., Zhang, X.-H., Osakabe, K., Tsai, C.-J., Joshi, C.P., and Chiang, V.L.** (1997). A novel multifunctional *O*-methyltransferase implicated in a dual methylation pathway associated with lignin biosynthesis in loblolly pine. Proc. Natl. Acad. Sci. USA **94,** 5431–5466.

**Li, L., Osakabe, Y., Joshi, C.P., and Chiang, V.L.** (1999). Secondary xylem-specific expression of caffeoyl-coenzyme A 3-*O*-methyltransferase plays an important role in the methylation pathway associated with lignin biosynthesis in loblolly pine. Plant Mol. Biol. **40,** 555–565.

**Li, L., Popko, J.L., Umezawa, T., and Chiang, V.L.** (2000). 5-Hydroxyconiferyl aldehyde modulates enzymatic methylation for syringyl monolignol formation: A new view of monolignol biosynthesis in angiosperms. J. Biol. Chem. **275,** 6537–6545.

**Lüderitz, T., and Grisebach, H.** (1981). Enzymic synthesis of lignin precursors: Comparison of cinnamoyl-CoA reductase and cinnamyl alcohol:$NADP^+$ dehydrogenase from spruce (*Picea abies* L.) and soybean (*Glycine max* L.). Eur. J. Biochem. **119,** 115–124.

**MacKay, J.J., Liu, W., Whetten, R., Sederoff, R.R., and O'Malley, D.** (1995). Genetic analysis of cinnamyl alcohol dehydrogenase in loblolly pine: Single gene inheritance, molecular characterization and evolution. Mol. Gen. Genet. **247,** 537–545.

**Mansell, R.L., Gross, G.G., Stöckigt, J., Franke, H., and Zenk, M.H.** (1974). Purification and properties of cinnamyl alcohol dehydrogenase from higher plants involved in lignin biosynthesis. Phytochemistry **13,** 2427–2435.

**Mansell, R.L., Babbel, G.R., and Zenk, M.H.** (1976). Multiple forms and specificity of cinnamyl alcohol dehydrogenase from cambial regions of higher plants. Phytochemistry **15,** 1849–1853.

**Musha, Y., and Goring, D.A.I.** (1975). Distribution of syringyl and guaiacyl moieties in hardwoods as indicated by ultraviolet microscopy. Wood Sci. Technol. **9,** 45–58.

**Nakano, J., and Meshitsuka, G.** (1992). The detection of lignin. In Methods in Lignin Chemistry, C.W. Dence and S.Y. Lin, eds (New York: Springer-Verlag), pp. 23–61.

**O'Malley, D., Porter, S., and Sederoff, R.R.** (1992). Purification, characterization, and cloning of cinnamyl alcohol dehydrogenase in loblolly pine (*Pinus taeda*). Plant Physiol. **98,** 1364–1371.

**Osakabe, K., Tsao, C.C., Li, L., Popko, J.L., Umezawa, T., Carraway, D.T., Smeltzer, R.H., Joshi, C.P., and Chiang, V.L.** (1999). Coniferyl aldehyde 5-hydroxylation and methylation direct syringyl lignin biosynthesis in angiosperms. Proc. Natl. Acad. Sci. USA **96,** 8955–8960.

**Parvathi, K., Chen, F., Guo, D., Blount, J.W., and Dixon, R.A.** (2001). Substrate preferences of *O*-methyltransferases in alfalfa suggest new pathways for 3-*O*-methylation of monolignols. Plant J. **25,** 193–202.

**Raven, J.A.** (1977). The evolution of vascular plants in relation to supracellular transport processes. In Advances in Botanical Research, H.W. Woolhouse, ed (London: Academic Press), pp. 153–219.

**Rolando, C., Monties, B., and Lapierre, C.** (1992). Thioacidolysis. In Methods in Lignin Chemistry, C.W. Dence and S.Y. Lin, eds (New York: Springer-Verlag), pp. 334–349.

**Ryser, U., and Keller, B.** (1992). Ultrastructural localization of a bean glycine-rich protein in unlignified primary walls of protoxylem cells. Plant Cell **4,** 773–783.

**Saka, S., and Goring, D.A.I.** (1985). Localization of lignin in wood cell walls. In Biosynthesis and Biodegradation of Wood Components, T. Higuchi, ed (New York: Academic Press), pp. 141–160.

**Saka, S., and Goring, D.A.I.** (1988). The distribution of lignin in white birch wood as determined by bromination with TEM-EDXA. Holzforschung **42,** 149–153.

**Samaj, J., Hawkins, S., Lauvergeat, V., Grima-Pettenati, J., and Boudet, A.M.** (1998). Immunolocalization of cinnamyl alcohol dehydrogenase 2 (CAD2) indicates a good correlation with cell-specific activity of CAD2 promoter in transgenic poplar shoots. Planta **204,** 437–443.

**Sarkanen, K.V., and Hergert, H.L.** (1971). Classification and distribution. In Lignins: Occurrence, Formation, Structure and Reaction, K.V. Sarkanen and C.H. Ludwig, eds (New York: Wiley-Interscience), pp. 43–94.

**Sarni, F., Grand, G., and Boudet, A.M.** (1984). Purification and properties of cinnamoyl-CoA reductase and cinnamyl alcohol dehydrogenase from poplar stems. Eur. J. Biochem. **139,** 259–265.

**Sato, Y., Watanabe, T., Komamine, A., Hibino, T., Shibata, D., Sugiyama, M., and Fukuda, H.** (1997). Changes in the activity and mRNA of cinnamyl alcohol dehydrogenase during tracheary element differentiation in zinnia. Plant Physiol. **113,** 425–430.

**Scurfield, G.** (1973). Reaction wood: Its structure and function. Science **179,** 647–655.

**Scurfield, G., and Bland, D.E.** (1963). The anatomy and chemistry of rubbery wood in apple variety Lord Lambourne. J. Hortic. Sci. **38,** 297–306.

**Somssich, I.E., Bollman, J., Hahlbrock, K., Kombrink, E., and Schulz, W.** (1989). Differential early activation of defense-related genes in elicitor-treated parsley cells. Plant Mol. Biol. **12,** 227–234.

**Somssich, I.E., Wernert, P., Kiedrowski, S., and Hahlbrock, K.** (1996). *Arabidopsis thaliana* defense-related protein ELI3 is an aromatic alcohol:$NADP^+$ oxidoreductase. Proc. Natl. Acad. Sci. USA **93,** 14199–14203.

**Stewart, D., Yahiaoui, N., McDougall, G.J., Myton, K., Marque, C., Boudet, A.M., and Haigh, J.** (1997). Fourier-transform infrared and Raman spectroscopic evidence for the incorporation of cinnamaldehydes into the lignin of transgenic tobacco (*Nicotiana*

*tabacum* L.) plants with reduced expression of cinnamyl alcohol dehydrogenase. Planta **201,** 311–318.

**Terashima, N., Fukushima, K., and Takabe, K.** (1986). Heterogeneity in formation of lignin: An autoradiographic study on the formation of guaiacyl and syringyl lignin in *Magnolia kobus*. Holzforschung **42,** 101–105.

**Towers, G.H.N., and Gibbs, R.D.** (1953). Lignin chemistry and the taxonomy of higher plants. Nature **172,** 25–26.

**Trotter, P.C.** (1990). Biotechnology in the pulp and paper industry: A review. Tech. Assoc. Pulp Paper Ind. J. **73,** 198–204.

**Tsai, C.-J., Popko, J.L., Mielke, M.R., Hu, W.-J., Podila, G.K., and Chiang, V.L.** (1998). Suppression of *O*-methyltransferase gene by homologous sense transgene in quaking aspen causes red-brown wood phenotypes. Plant Physiol. **117,** 101–112.

**Umezawa, T.** (1994). Lignan. In Wood Molecular Biology, T. Higuchi, ed (Tokyo: Buneido Publishing), pp. 140–145.

**Van Doorsselaere, J., Baucher, M., Feuillet, C., Boudet, A.M., Van Montagu, M., and Inzé, D.** (1995). Isolation of cinnamyl alcohol dehydrogenase cDNAs from two important economic species: Alfalfa and poplar. Demonstration of a high homology of the gene within angiosperms. Plant Physiol. Biochem. **33,** 105–109.

**Wardrop, A.B.** (1971). Occurrence and formation in plants. In Lignins: Occurrence, Formation, Structure and Reaction, K.V. Sarkanen and C.H. Ludwig, eds (New York: Wiley-Interscience), pp. 19–42.

**Wardrop, A.B.** (1981). Lignification and xylogenesis. In Xylem Cell Development, J.R. Barnett, ed (Tunbridge Wells, UK: Castle House Publications), pp. 115–152.

**Wardrop, A.B., and Dadswell, H.E.** (1952). The cell wall structure of xylem parenchyma. Aust. J. Sci. Res. Ser. B Biol. Sci. **5,** 223–236.

**Wardrop, A.B., and Davies, G.W.** (1964). The structure of reaction wood: The structure and differentiation of compression wood. Aust. J. Bot. **12,** 24–38.

**Wengenmayer, H., Ebel, J., and Grisebach, H.** (1976). Enzymic synthesis of lignin precursors: Purification and properties of a cinnamoyl-CoA:NADPH reductase from cell suspension cultures of soybean. Eur. J. Biochem. **65,** 529–536.

**Whetten, R., and Sederoff, R.** (1995). Lignin biosynthesis. Plant Cell **7,** 1001–1013.

**Whetten, R.W., MacKay, J.J., and Sederoff, R.R.** (1998). Recent advances in understanding lignin biosynthesis. Annu. Rev. Plant Physiol. Plant Mol. Biol. **49,** 585–609.

**Wittich, P.E., de Heer, R.F., Cheng, X.F., Kieft, H., Colombo, L., Angenent, G.C., and van Lammeren, A.M.M.** (1999). Immunolocalization of the petunia floral binding protein 7 and 11 during seed development in *Petunia hybrida*. Protoplasma **208,** 224–229.

**Wu, L., Joshi, C.P., and Chiang, V.L.** (2000). A xylem-specific cellulose synthase gene from aspen is responsive to tension stress. Plant J. **22,** 495–502.

**Wyrambik, D., and Grisebach, H.** (1975). Purification and properties of isoenzymes of cinnamyl-alcohol dehydrogenase from soybean cell-suspension cultures. Eur. J. Biochem. **59,** 9–15.

**Wyrambik, D., and Grisebach, H.** (1979). Enzymic synthesis of lignin precursors: Further studies on cinnamyl-alcohol dehydrogenase from soybean cell-suspension cultures. Eur. J. Biochem. **97,** 503–509.

**Ye, Z.H., Kneusel, R.E., Matern, U., and Varner, J.E.** (1994). An alternative methylation pathway in lignin biosynthesis in Zinnia. Plant Cell **6,** 1427–1439.

**Zhang, X.-H., and Chiang, V.L.** (1997). Molecular cloning of a 4-coumarate:coenzyme A ligase (4CL) in loblolly pine and the roles of this enzyme in the biosynthesis of lignin in compression wood. Plant Physiol. **113,** 65–74.

**Zhong, R., Morrison, H., Negrel, J., and Ye, Z.H.** (1998). Dual methylation pathways in lignin biosynthesis. Plant Cell **10,** 2033–2045.

**Zinser, C., Ernst, D., and Sandermann, H., Jr.** (1998). Induction of stilbene synthase and cinnamyl alcohol dehydrogenase mRNAs in Scots pine (*Pinus sylvestris* L.) seedlings. Planta **204,** 169–176.